

Modeling of Geochemical Processes Occurred during the Formation of the Schlema Deposit, Erzgebirge.

II. Formation of Pre-Uranium Veins

Vikt. L. Barsukov

*Vernadsky Institute of Geochemistry and Analytical Chemistry, Russian Academy of Sciences,
ul. Kosygina 19, Moscow, 119991 Russia*

Received April 19, 2005

Abstract—By means of computer modeling, it was shown that the pre-uranium quartz and quartz–sulfide veins of the Schlema deposit with their typomorphic assemblages could be formed at the expense of cooling of hot pore solutions from the Aue granite cupola underlying the mineralized zones. As was shown previously [1], the ore metal content of these pore solutions changes with decreasing temperature and pressure in the granite–water system and an increase in the intensity of granite “flushing” with a water phase. The dependence of the composition of precipitated material on the proportions of chlorides and carbon dioxide in the pore solutions was evaluated in the models. It was shown that silica mobilization from the granite and redeposition were accompanied by the oxidation of ferrous iron in the granite and extraction of sulfide sulfur in molal amounts similar to or even higher than those of silica. This provided conditions for uranium migration after these stages and formation of hydrothermal uranium ores.

DOI: 10.1134/S0016702906120044

INTRODUCTION

In the first paper of this series [1], we considered interactions between the granites of the Aue cupola and a water phase infiltrated through the granites at T – P conditions from 400°C and 3.0–1.5 kbar to 140°C and 2.0–0.5 kbar. These interactions resulted in a weak hydrothermal alteration of the mineral and chemical composition of the granite and evolution of the composition and properties of equilibrium pore solutions, including changes in the release of metals from the granite into these solutions. This paper focuses on the investigation of the fate of pore solutions from the Aue granite cupola. According to the models of Vlasov [2] and Acheev [3], the system of steeply dipping fractures above the slope of the Aue cupola in which filling veins were formed during sequential stages of mineralization in the Schlema uranium deposit drained the border zone of the cupola and had to be fed by its pore solutions. Hence, the evolutionary trends in the composition of pore solutions with decreasing T and P observed in the models [1] reflect also gradual changes in the composition and properties of ascending solutions arriving from the pore space of the granite into these fracture systems and depositing gangue and ore materials. The high-temperature pore solutions that migrated from the granite into the ore field could potentially form the early pre-uranium veins of the quartz and quartz–sulfide stages of hydrothermal processes at Schlema.

The veins of these premineralization stages are of little interest by themselves, because their analogs are widespread in the Earth’s crust and were described in

detail in hundreds of publications. Therefore, we did not attempt to discover something fundamentally new supplementing the available information on the genesis of these very common objects in hydrothermal systems. However, the fact is that such veins in Schlema and in most uranium vein deposits *typically predate uranium mineralization*. It is well known that they always occupy the same place in the sequence of hydrothermal stages in all uranium deposits of the world: quartz (or quartz–silicate) stage → quartz–sulfide (occasionally, carbonate–sulfide) stage → quartz–carbonate–pitchblende stage → later stages. Since this sequence is persistent, it probably bears some genetic geochemical meaning. Therefore, the goal of this study was not merely to model the process of formation of these particular veins. We formulated another problem: to attempt to understand, *why the deposition of primary uranium ores at Schlema (and almost everywhere) was preceded by the formation of these premineralization quartz and quartz–sulfide veins. Were these premineralization hydrothermal processes at Schlema (as well as in other complexes) necessary for the subsequent formation of uranium ores and, if yes, in which way?* It is obvious that the analysis of these questions requires a cursory description of these veins and modeling of some features of their formation.

Compared with part I of this study [1], the list of components of the system was expanded by introducing four new components: Mn, Ti, F, and P. In this paper, physicochemical equilibria are modeled using the program complex Hch by Yu.V. Shvarov with the

thermodynamic database UNITERM [4, 5] in a heterogeneous system composed of 23 independent components: H–O–K–Na–Ca–Mg–Mn–Fe–Al–Ti–Si–Cl–F–S–C–P–W–Sn–Mo–Pb–Zn–Cu–U. This system is described by 83 solid phases and 184 aqueous species.

EARLY QUARTZ VEINS

The fissure quartz veins are not the earliest SiO₂ concentrators within the Schlema ore field. Before the development of these veins and fractures in which they were formed, all the rocks of the near contact zone of the Aue granite cupola and, to a lesser extent, the apical part of the cupola were enriched in newly formed quartz occurring as small isolated lenses, clots, schlieren, and short veinlets. Most of them were related to the contact metamorphism of rocks and formed at 500–400°C and 3–2 kbar [6, 7], probably at the expense of the redistribution of rock-forming quartz. Various possible reasons for silica redeposition under hydrothermal conditions were discussed in the literature: a gradient in chemical potential owing to the difference in fluid pressure between the pore space of rocks and developing fractures [8–10], difference in free energy between the stressed quartz grains of rock and undeformed newly formed quartz grains in open cavities [11, 12], and others. It cannot be excluded that these processes played a role in the local redistribution of SiO₂ in the contact zone of the Aue granite cupola. However, the extensive silicification of rocks in the near contact zone of the granite massif [13] suggests a considerable influx of silica into this region, which can be the subject of special investigation. The focus of the present study is not the frontal silicification of rocks in a narrow zone of near-granite contact metamorphism and not the redistribution of silica during the formation of metamorphic quartz lenses, schlieren, and “closed” veinlets, which are abundant in this aureole. We consider here steeply dipping veins of the early quartz stage, which extend far from the granite and were formed by filling the free space of fissures with the material that was obviously supplied from an external source.

Composition of Early Quartz Veins

The quartz veins are from a few decimeters to a few meters thick and extend up to 500 m along strike and up to 150–500 m down dip in the rocks of the granite roof at a distance of up to 500–1000 m from the granite and, occasionally, in the border zone of the Aue granite cupola. According to Acheev [3], quartz veins account for 19.8% of the total thickness (volume) of the vein bodies of all stages of the hydrothermal process at a horizon of –810 m relative to the MS level (Markus Semmler gallery is a convenient zero depth for the Schlema deposit, 330 m above sea level), which was selected by him for the calculation of quantitative relationships between various mineralization stages.

The veins are composed mainly of massive milk-white quartz, with minor fluorite, feldspars, muscovite, apatite, rutile, tourmaline (schorl), actinolite (tremolite), chlorite, and other mafic minerals. Varying amounts of pyrite, arsenopyrite, loellingite, pyrrhotite, and molybdenite are common. Pb–Zn–Cu sulfides are less abundant. Magnetite, ilmenite, cassiterite, and wolframite occur occasionally. After the recrystallization of the quartz filling, the primary texture of the veins is practically obliterated, and they show now a massive secondary texture. Sometimes, the veins are divided into decimeter-sized and larger blocks, the boundaries of which are outlined by black stringers of graphitic material, which are probably products of quartz self-purification during recrystallization. Shadow relics of banded structures were observed in some veins. They can be considered as evidence for multiple quartz precipitation. The investigation of fluid inclusions in these *recrystallized* early quartz veins of Schlema showed that the inclusions were formed at 350–300°C and a pressure of about 1 kbar [6]. Identical temperatures were obtained from the oxygen isotope systematics of these veins [7].

Two observations are important for the reconstruction of the physicochemical conditions of early quartz vein formation. First, the distribution of veins, their composition, and structure *are independent* of the composition of the environment. Without any change in composition or thickness, they cross the boundaries of the “productive sequence” of Schlema¹ [2], pass from quartz–sericite phyllites into metadiabases, then into carbonaceous shales, then again into quartz–sericite schists, etc. Second, the rocks of the ore field did not experience significant metasomatic alterations near the quartz veins. This evidently suggests that quartz precipitation from silica-bearing solutions was accompanied by either a *weak chemical interaction* between these solutions and the environment or *no interaction at all*.

The main factor of long-distance silica transport and formation of fissure quartz veins was the cooling of ascending silica-saturated aqueous solutions. It has long been known that quartz solubility in aqueous solutions is essentially independent either of the concentration of dissolved salts or pH and Eh of the solution [14, 15]. Exchange chemical reactions between aqueous solutions and the enclosing rocks accompanied by some changes in the salt composition, alkalinity, and redox potential of the solutions cannot result in extensive silica precipitation. In contrast, quartz solubility decreases substantially with the cooling of solutions. Therefore, “if a fluid flow is concentrated in open fissures, this should inevitably result in the formation of quartz veins in the cases when the rocks are rich in sil-

¹ A sequence of Silurian–Devonian rocks (dark-colored carbon- and pyrite-bearing phyllites, carbonaceous schists, skarns, and metadiabases), which proved to be most favorable for uranium precipitation by hydrothermal solutions and contain about 95% of uranium vein ores.

ica, and the flow is directed from a hot zone to a cooler one" [10]. In our case, we can consider the cooling Aue granite cupola as a hot zone and the overlying rocks within the limits of the Schlema ore field as a colder zone.

In hydrothermal systems, the temperature gradient may be equal to or higher than a normal geothermal gradient of 35°C/km. "The high temperatures encountered in wells in such areas as Wairakei, New Zealand and the Salton Sea, California, suggest that thermal gradients during ore deposition may sometimes have been as large as 100°C/km" [14]. The situation with pressure gradient is similar. "The near-surface pressure gradient in most wells is nearly hydrostatic. In deep wells the pressure gradient approaches the lithostatic gradient, and it seems likely that during ore deposition the pressure gradient lies between these two extreme limits" [14]. With application to Schlema, this means that, if the temperature of formation of early quartz veins 0.5–1.0 km above the granite roof was really 350–300°C at 1.5–1.0 kbar [6, 7], the temperature of the granite within the Aue cupola, i.e., 2–4 km below the region of quartz precipitation, as well as the temperature of its pore solutions could be as high at that time as 500–400°C, and the pressure could also be higher, probably up to 3–2 kbar.

There is no need to demonstrate by models the long established and universally known effects of quartz precipitation from solutions during their cooling. We will draw the attention of the reader primarily not on the behavior of Si during the formation of the early quartz veins of Schlema but rather on the behavior of accompanying components.

Models of Saturation of the Pore Solution of the Aue Granite in Silica and Other Components

As was shown in [1], high-temperature pore solutions in thermodynamic equilibrium with the Aue granite are silica-bearing alkali chloride solutions, in which the major fraction of carbon dioxide occurs as undissociated neutral molecules, and almost all sulfur occurs as hydrosulfide. Since the granite–water system was extended in this study by introducing four new components, the bulk composition of pore solutions of the granite was recalculated by the new models of thermodynamic equilibration at high T and P with *pure water and an aqueous phase with varying (NaCl + KCl)/H₂CO₃ ratio (from 11 to 0.11)*. All other macro- and microcomponents of the pore solutions are extracted by water and chloride–carbon dioxide aqueous phases only from the granite interacting with them. The models imitated reactions between 1 kg H₂O solution (W) and 10 kg (R) of unaltered granite from the lower levels of the Aue cupola. Our experience indicates that such R/W ratios are sufficient for reaching the plateau of all variable characteristics of the granite–solution system: mineral and chemical compositions of the solid phase, composition of solutions, their ionic strength, alkalinity, and redox potential; in other words,

they are sufficient for the appearance of all the characteristics of granite–solution equilibration. Some examples of the compositions of equilibrium pore solutions from granites obtained in high- T and high- P models are shown in Tables 1–3.

As can be seen from these tables, the concentrations of major components of pore solutions evidently depend, at constant pressure, on the preset Cl/C ratio. It is true that almost all the components, including Si, show molar concentrations varying as a function of Cl/C within one order of magnitude, and only the concentration of Fe decreases with decreasing m_{Cl} by three orders of magnitude. Similar to iron, the concentrations of a number of ore elements are proportional to the bulk chloride concentration in the solution, which is understandable, considering that the chloride complexes of Pb, Zn, and Sn account for a significant fraction of the dissolved metals at high temperatures. In contrast, the concentration of Cu in the pore solutions increases with decreasing Cl/C. This effect is evidently due to an increase in pH and transformation of part of dissolved copper from hydrosulfide complexes (its chloride complexes are less important) into hydroxy complexes [1]. The concentrations of Mo and W are also inversely proportional to ΣCl . These metals are transported mainly as the MoO₄²⁻ and HWO₄⁻ anions in the models. The concentration of H₂CO₃ exerts a minor influence on the behavior of dissolved metals, probably because it is practically undissociated at high T and P and does not occur in the composition of the main dissolved species of major and trace components of the system. A notable fact is that the solubility of silica, as well as sulfur and other components, is *higher in pure water than in the model salt solutions*. It is also important that at a certain temperature and Cl/C proportions in the solution, the concentrations of major and trace components are affected by changes in pressure in the granite–solution system, which is illustrated for silica and metals in Tables 4 and 5, respectively.

The extension of the system (in particular, introduction of Mn) slightly changed the composition of pore solutions compared to the models reported in [1]. The behavior of ore elements was also affected. For instance, huebnerite instead of ferberite became a solid phase of W in the granite. The solubility of huebnerite in the model appeared to be lower, which decreased the concentration of W in the new model pore solutions by almost two orders of magnitude. The concentrations of Sn and Cu also decreased, but the reason for this effect is less obvious than in the case of W. The concentrations of Pb, Zn, Mo, and U in the model pore solutions remained practically the same as in part I of this study [1].

The pore solutions whose salt composition is shown in Tables 1–3 and in part in Tables 4 and 5 are products of interaction between initial water phases without ore metals and the Aue granite. This interaction caused a slight change in the major-element composition of the granite (such changes were aptly called "dispersed

Table 1. Compositions of pore solutions obtained by the equilibration of granite GR14 at 400°C and 3 kbar with an aqueous phase depending on the Cl/C ratio in it, mol/kg H₂O

Cl/C	11	2.2	1.1	0.55	0.11	H ₂ O
H	6.066E-01	1.411E+00	2.416E+00	2.418E+00	2.422E+00	4.219E-01
O	8.414E-01	2.052E+00	3.565E+00	3.568E+00	3.575E+00	6.012E-01
K	2.108E-01	2.109E-01	2.110E-01	1.081E-01	3.249E-02	2.183E-02
Na	9.488E-01	9.513E-01	9.543E-01	5.070E-01	1.536E-01	7.831E-02
Ca	4.509E-05	4.560E-05	4.623E-05	2.222E-05	8.327E-05	6.048E-06
Mg	5.610E-05	5.650E-05	5.701E-05	3.082E-05	1.911E-05	1.714E-05
Mn	1.193E-04	1.220E-04	1.254E-04	5.983E-05	2.454E-05	1.748E-05
Fe	1.259E-03	1.248E-03	1.235E-03	2.987E-04	1.091E-05	1.658E-06
Al	1.974E-06	1.982E-06	1.993E-06	1.962E-06	1.924E-06	1.898E-06
Ti	3.834E-06	3.805E-06	3.769E-06	3.694E-06	3.457E-06	3.537E-06
Si	4.797E-02	4.764E-02	4.723E-02	4.819E-02	4.968E-02	5.177E-02
Cl	1.111E+00	1.111E+00	1.111E+00	5.555E-01	1.111E-01	0
F	1.645E-02	1.656E-02	1.669E-02	1.882E-02	2.694E-02	3.642E-02
S	3.009E-02	3.009E-02	3.011E-02	3.075E-02	3.273E-02	4.598E-02
C	1.928E-01	5.967E-01	1.102E+00	1.102E+00	1.102E+00	9.186E-02
P	2.167E-06	2.181E-06	2.199E-06	3.857E-06	1.284E-05	2.863E-05
W	9.430E-06	9.521E-06	9.634E-06	1.669E-05	5.421E-05	1.222E-04
Sn	3.638E-05	3.624E-05	3.606E-05	2.330E-05	7.235E-06	2.815E-16
Mo	8.973E-10	9.045E-10	9.134E-10	1.319E-09	2.845E-09	6.169E-09
Pb	1.261E-05	1.254E-05	1.246E-05	6.982E-06	6.553E-06	6.529E-06
Zn	7.181E-05	7.082E-05	6.960E-05	8.590E-06	2.999E-06	2.771E-06
Cu	9.815E-07	9.831E-07	9.851E-07	1.436E-06	3.138E-06	5.137E-06
U	6.713E-11	6.765E-11	6.836E-11	6.803E-11	7.933E-11	8.028E-11
I	0.791	0.793	0.796	0.456	0.152	0.086
pH	5.343	5.345	5.348	5.541	5.937	6.183
Eh, mV	-624	-624	-624	-653	-713	-747

muscovitization” by Zaraiskii [16]) and extraction from it of trace ore elements [1, 17, 18]. Their cation composition is dominated by Na and K. The concentrations of major divalent components decrease at 500–400°C in the sequence Fe → Mn → Mg → Ca. Among anion-forming components, carbon dioxide and chlorides are predominant, and other components form the following sequence of decreasing concentration Si → S → F → P. The concentration of uranium in the solutions is E–09 to E–11 mol/kg H₂O, and the total concentration of other ore elements is up to 50–70 mg/kg H₂O.

The cooling of such solutions and its consequences are analyzed in the following series of thermodynamic models.

Models of Cooling of High-Temperature Solutions and Quartz Precipitation

Processes related to the transition from the initial temperature and pressure of high-temperature pore solutions to the *T-P* conditions of the early quartz stage were investigated in 56 models, using the compositions of the initial pore solutions from Tables 1–3 as input parameters. We modeled disturbances in thermodynamic equilibria *in response to a decrease in T and P* only up to the values characteristic of the processes of

formation of the early quartz veins of Schlema, *without chemical exchange reactions between the solution and the environment*.

A general consequence of the cooling of high-temperature pore solutions of granite to 350–300°C and decompression to 2–1 kbar is the precipitation of significant amounts of quartz. The dynamics of this precipitation is illustrated by Fig. 1. The upper panel (Fig. 1a) shows variations in the bulk concentration of dissolved silica in the model pore solutions owing to a decrease in *T* and *P* in the system. Similar to the initial solutions, the silica solubility is only slightly dependent on the Cl/C ratio (Tables 1–5). All variations in silica solubility related to changes in Cl/C are confined to a narrow range between the maximum Si concentration in pure H₂O and the minimum Si concentration in the solutions with Cl/C ≈ 1. The effect of pressure is more significant. The upper of the two ranges in Fig. 1a corresponds to a pressure of 3 kbar at 500–350°C, and the lower one corresponds to 2 kbar. Figure 1b shows the amount of precipitated SiO₂(cr) during cooling. Variant I refers to solutions with an initial pressure of 3 kbar. Calculations 1, 2, and 3 correspond to solution cooling to 350°C from initial temperatures of 500, 450, and 400°C, respectively; and calculations 4, 5, and 6 show the same solutions cooled to 300°C. Variant II was calculated for

Table 2. Compositions of pore solutions obtained by the equilibration of granite GR14 at 450°C and 3 kbar with an aqueous phase depending on the Cl/C ratio in it, mol/kg H₂O

Cl/C	11	2.2	1.1	0.55	0.11	H ₂ O
H	7.628E-01	1.568E+00	2.575E+00	2.581E+00	2.595E+00	5.975E-01
O	8.760E-01	2.086E+00	3.598E+00	3.602E+00	3.611E+00	5.948E-01
K	2.047E-01	2.074E-01	2.074E-01	1.037E-01	2.658E-02	1.089E-02
Na	9.304E-01	9.311E-01	9.321E-01	4.857E-01	1.309E-01	5.010E-02
Ca	3.130E-05	3.150E-05	3.175E-05	1.718E-05	7.941E-06	5.965E-06
Mg	7.346E-05	7.396E-05	7.459E-05	4.329E-05	2.885E-05	2.528E-05
Mn	1.547E-04	1.553E-04	1.559E-04	6.259E-05	6.589E-05	1.920E-05
Fe	2.297E-03	2.279E-03	2.258E-03	5.799E-04	2.281E-05	3.009E-06
Al	7.217E-06	7.248E-06	7.287E-06	7.186E-06	7.065E-06	6.921E-06
Ti	2.178E-06	2.162E-06	2.142E-06	2.106E-06	1.993E-06	1.920E-06
Si	6.646E-02	6.599E-02	6.543E-02	6.662E-02	6.837E-02	7.139E-02
Cl	1.111E+00	1.111E+00	1.111E+00	5.555E-01	1.111E-01	0
F	2.174E-02	2.187E-02	2.202E-02	2.373E-02	3.085E-02	4.242E-02
S	5.752E-02	5.756E-02	5.760E-02	5.958E-02	6.501E-02	7.140E-02
C	1.928E-01	5.967E-01	1.102E+00	1.102E+00	1.102E+00	9.184E-02
P	1.644E-06	1.655E-06	1.699E-06	2.700E-06	8.268E-06	2.339E-05
W	9.886E-06	9.965E-06	1.006E-05	1.553E-05	4.504E-05	1.213E-04
Sn	8.047E-05	8.021E-05	7.988E-05	5.213E-05	1.672E-05	6.512E-16
Mo	1.053E-09	1.044E-09	1.055E-09	1.472E-09	3.150E-09	6.282E-09
Pb	3.432E-05	3.421E-05	3.406E-05	2.358E-05	2.328E-05	2.460E-05
Zn	2.161E-04	2.133E-04	2.098 E-04	2.544E-05	9.001E-06	8.903E-06
Cu	3.129E-06	3.134E-06	3.140E-06	4.496E-06	9.875E-06	1.937E-05
U	3.162E-10	3.160E-10	3.158E-10	1.704E-10	1.619E-10	1.904E-10
I	0.674	0.676	0.678	0.389	0.122	0.05
pH	5.277	5.279	5.282	5.47	0.878	6.208
Eh, mV	-685	-685	-685	-716	-781	-835

the same temperature variations with solutions formed at an initial pressure of 2 kbar. Thus, the maximum silica precipitation of almost 5 g SiO₂(cr) per 1 kg H₂O was obtained when the solution equilibrated with granite at 500°C and 3 kbar was immediately (without Si loss along its way) cooled to the lower temperature boundary of the quartz stage (300°C at 1.5 kbar).

The significant disturbances of physicochemical equilibria during the cooling and decompression of initial solutions resulted in the coprecipitation with quartz of minor amounts of other solid phases of various chemical classes.² The most abundant ore minerals in the model precipitates are sulfides: pyrite, sphalerite, and galena; less common are chalcopyrite, bornite, covellite, troilite, and molybdenite. There are also other ore minerals in the precipitate, including wolframite (ferberite or huebnerite if Mn is present in the system), cassiterite,

² As and B were not included into the system because of the lack of thermodynamic data for their solid phases. That is why the model precipitates contained no arsenopyrite and tourmaline, in contrast to the prototypes, the real veins of the early quartz stage of Schlema.

and very small (<0.001 wt %) amounts of U minerals, uraninite or titanates, UTiO₄(cr) and U(TiO₃)₂(cr). Among the gangue minerals cogenetic with quartz, fluorite and F-apatite are most abundant; trace amounts of microcline (occasionally, albite), epidote, amphiboles (Fe-tremolite, actinolite, and tremolite), phlogopite, muscovite, chlorites, rhodonite, pyrophyllite, wollastonite, and rutile were also detected. In some models, chloride-poor initial solutions precipitate small amounts of graphite during cooling to 320–300°C and a pressure decrease to 1.5 kbar.

In order to better illustrate the results of modeling, we selected from Tables 1–5 solutions with a medium initial temperature of 450°C and 3 kbar. Their cooling and decompression to the parameters of the quartz hydrothermal stage of Schlema resulted in the formation of a precipitate, which is shown in Fig. 2. Its y axis shows the mass proportions of minerals in the precipitates obtained in *discrete calculations* for the combinations of *T* and *P* indicated along the *x* axis (with a step of 10°C and 100 bar). In this and further diagrams, we constructed only the *fields of solid phases coprecipitat-*

Table 3. Compositions of pore solutions obtained by the equilibration of granite GR14 at 500°C and 3 kbar with an aqueous phase depending on the Cl/C ratio in it, mol/kg H₂O

Cl/C	11	2.2	1	0.55	0.11	H ₂ O
H	1.076E+00	1.883E+00	2.893E+00	2.904E+00	2.929E+00	9.334E-01
O	1.008E+00	2.220E+00	3.736E+00	3.741E+00	3.752E+00	7.291E-01
K	2.124E-01	2.123E-01	2.123E-01	1.103E-01	3.305E-02	1.672E-02
Na	9.428E-01	9.432E-01	9.436E-01	4.955E-01	1.383E-01	5.584E-02
Ca	2.453E-05	2.466E-05	2.483E-05	1.557E-05	8.894E-06	7.166E-06
Mg	1.050E-04	1.057E-04	1.066E-04	6.557E-05	4.694E-05	4.200E-05
Mn	2.603E-04	2.599E-04	2.594E-04	8.668E-05	3.252E-05	2.578E-05
Fe	3.312E-03	3.289E-03	3.262E-03	8.855E-04	4.080E-05	6.225E-06
Al	2.646E-05	2.658E-05	2.672E-05	2.640E-05	2.602E-05	2.553E-05
Ti	1.400E-06	1.390E-06	1.377E-06	1.361E-06	1.302E-06	1.269E-06
Si	8.935E-02	8.872E-02	8.796E-02	8.938E-02	9.122E-02	9.434E-02
Cl	1.114E+00	1.114E+00	1.114E+00	5.572E-01	1.115E-01	0
F	3.339E-02	3.357E-02	3.378E-02	3.496E-02	3.994E-02	4.711E-02
S	1.690E-01	1.691E-01	1.692E-01	1.738E-01	1.851E-01	1.964E-01
C	1.933E-01	5.984E-01	1.105E+00	1.105E+00	1.105E+00	9.212E-02
P	1.147E-06	1.153E-06	1.162E-06	1.683E-06	4.067E-06	9.265E-06
W	1.238E-05	1.244E-05	1.251E-05	1.627E-05	3.371E-05	7.084E-05
Sn	9.898E-05	9.868E-05	9.832E-05	6.388E-05	2.038E-05	1.873E-15
Mo	2.167E-09	2.189E-09	2.214E-09	2.963E-09	5.702E-09	1.020E-08
Pb	7.893E-05	7.874E-05	7.850E-05	5.878E-05	5.825E-05	6.089E-05
Zn	6.459E-04	6.384E-04	6.292E-04	7.315E-05	2.160E-05	2.100E-05
Cu	8.773E-06	8.776E-06	8.780E-06	1.222E-05	2.475E-05	4.462E-05
U	6.669E-09	6.633E-09	6.587E-09	1.408E-09	2.583E-10	2.691E-10
I	0.585	0.587	0.589	0.347	1.119	0.055
pH	5.242	5.244	5.246	5.422	5.793	6.082
Eh, mV	-735	-735	-736	-765	-828	-878

Table 4. Concentration of Si in high-temperature pore solutions from the granite of the Aue cupola at various *T*, *P*, and MCl/CO₂ ratios

		Mole Si/kg H ₂ O × 10 ⁻²					
M _{Cl} /M _C		11	2	1.1	0.55	0.11	H ₂ O
Cl, mol		1.1	1.1	1.1	0.55	0.11	0
CO ₃ , mol		0.1	0.55	1	1	1	0
500°C	3 kbar	8.935	8.887	8.769	8.938	9.122	9.434
	2 kbar	6.669	6.526	6.595	6.684	6.771	6.941
450°C	3 kbar	6.646	6.599	6.543	6.682	6.837	7.139
	2 kbar	5.043	5.008	4.965	5.030	5.119	5.281
400°C	3 kbar	4.781	4.764	4.723	4.819	4.968	5.177
	2 kbar	3.657	3.631	3.600	3.660	3.729	3.858
		Gram SiO ₂ /kg H ₂ O					
M _{Cl} /M _C		11	2	1.1	0.55	0.11	H ₂ O
500°C	3 kbar	5.366	5.337	5.289	5.368	5.479	5.666
	2 kbar	4.005	3.919	3.961	4.014	4.066	4.169
450°C	3 kbar	3.992	3.963	3.930	4.096	4.106	4.288
	2 kbar	3.029	3.008	2.982	3.026	3.074	3.172
400°C	3 kbar	2.871	2.861	2.837	2.894	2.984	3.109
	2 kbar	2.196	2.181	2.162	2.198	2.240	2.317

Table 5. Concentrations of ore components in the high-temperature pore solutions of the Aue granite under various P - T conditions and four preset Cl/C ratios in them, mol/kg H₂O

Cl/C	T , °C	P , kbar	W	Sn	Mo	Pb	Zn	Cu	U
11	500°C	3	1.24E-05	9.90E-05	2.17E-09	7.89E-05	6.46E-04	8.77E-06	6.67E-09
		2	2.12E-05	4.60E-05	5.51E-10	9.67E-05	4.27E-03	3.31E-06	2.54E-07
	450°C	3	9.89E-06	8.05E-05	1.03E-09	3.43E-05	2.16E-04	3.13E-06	3.16E-10
		2	7.85E-06	4.18E-05	2.78E-10	4.39E-05	1.10E-03	1.26E-06	5.19E-09
	400°C	3	9.43E-06	3.64E-05	8.97E-10	1.26E-05	7.18E-05	9.81E-07	6.71E-11
		2	4.08E-06	1.6E-05	3.88E-10	1.82E-05	3.17E-04	4.17E-07	2.24E-10
1.1	500°C	3	1.25E-05	9.83E-05	2.21E-09	7.85E-05	6.29E-04	8.78E-06	6.59E-09
		2	2.11E-05	4.58E-05	5.61E-10	9.59E-05	4.17E-03	3.31E-06	2.51E-07
	450°C	3	1.01E-05	7.99E-05	1.06E-09	3.41E-05	2.10E-04	3.14E-06	3.16E-10
		2	7.86E-06	4.16E-05	2.82E-10	4.34E-05	1.07E-03	1.27E-06	5.12E-09
	400°C	3	9.63E-06	3.61E-05	9.13E-10	1.25E-05	6.96E-05	9.85E-07	6.84E-11
		2	4.13E-06	1.59E-05	3.95E-10	1.79E-05	3.07E-04	4.19E-07	2.25E-10
0.11	500°C	3	3.37E-05	2.04E-05	5.7E-09	5.83E-05	2.16E-05	2.48E-05	2.58E-10
		2	2.47E-05	8.34E-06	1.45E-09	4.95E-05	3.11E-05	8.13E-06	1.62E-09
	450°C	3	4.5E-05	1.67E-05	3.15E-09	2.33E-05	9.0E-06	9.87E-06	1.62E-10
		2	1.52E-05	7.13E-06	1.05E-09	1.95E-05	1.11E-05	3.58E-06	2.89E-10
	400°C	3	5.42E-05	7.24E-06	2.84E-09	6.55E-06	3.0E-06	3.14E-06	7.93E-11
		2	1.54E-05	3.31E-06	1.12E-09	5.53E-06	3.46E-06	1.29E-06	1.43E-10
H ₂ O	500°C	3	7.08E-05	1.87E-15	1.02E-08	6.09E-05	2.1E-05	4.46E-05	2.69E-10
		2	3.35E-05	7.02E-16	2.85E-09	5.27E-05	2.71E-05	1.69E-05	4.33E-10
	450°C	3	1.21E-04	6.51E-16	6.28E-09	2.46E-05	8.9E-06	1.94E-05	1.90E-0
		2	4.13E-05	2.02E-16	2.59E-09	2.1E-05	1.03E-05	8.79E-06	3.16E-10
	400°C	3	0.000122	2.81E-16	6.16E-09	6.53E-06	2.77E-06	5.14E-06	8.03E-11
		2	4.86E-05	9.73E-17	2.48E-09	5.9E-06	3.11E-06	2.85E-06	1.64E-10

ing with quartz. The field above these accessory phases of precipitate, up to 100 wt %, corresponds to quartz. As can be seen from Fig. 2, although the composition of initial solutions was only slightly dependent on Cl/C, the composition of precipitate is much more sensitive to this ratio. The cooling of *chloride-dominated solutions* (Cl/C \approx 0.11) produced a precipitate with 91–93 wt % quartz and 9–7 wt % cogenetic solid phases (Fig. 2a). The latter are strongly dominated by pyrite; sphalerite and galena occur in smaller amounts. In addition to sulfides, the model precipitate contains minor wolframite, cassiterite, fluorite, F-apatite, and other minerals accounting together for about 0.2 wt %. Under the same conditions, the precipitate produced by a *chloride-poor solution* (Cl/C \approx 11) (Fig. 2b) contained only 0.35–0.20 wt % of minerals coprecipitating with quartz at the expense of a sharp decrease in the precipitation of sulfides. The masses of wolframite, cassiterite, galena, and fluorite changed only slightly compared with Fig. 2a, but their relative fraction among the accessory phases of the precipitate increased (wolframite even dominated among them at 350–320°C). Finally, *chloride-free solution* (obtained by equilibration of granite with pure H₂O, which extracted

E–02 mol CO₂/kg H₂O from the rock) transported and precipitated almost pure quartz (99.82 wt % of the precipitate) upon cooling (Fig. 2c). The cogenetic accessories are dominated by wolframite at all temperatures (its mass is 1.5–2.0 times higher than in Fig. 2b).

It should be noted that for each Cl/C– T – P combination in our models, the *average composition of precipitate* from a particular cooling solution was determined. The spatial distribution of various components and solid phases of the precipitate was not considered. In nature such precipitates are rarely homogeneous. A real vein may have a monomineralic quartz composition at one site and contain significant amounts of sulfides or fluorite at another site. There are numerous factors responsible for such local heterogeneities in veins, and they were not specially investigated. Nonetheless, our models give some hints to these factors. In particular, Fig. 2 shows changes in the composition of precipitate owing to possible variations in chloride concentration in space and time. It is also conceivable that the T and P conditions of the sources of silica-bearing solutions were variable throughout the Aue granite cupola. For

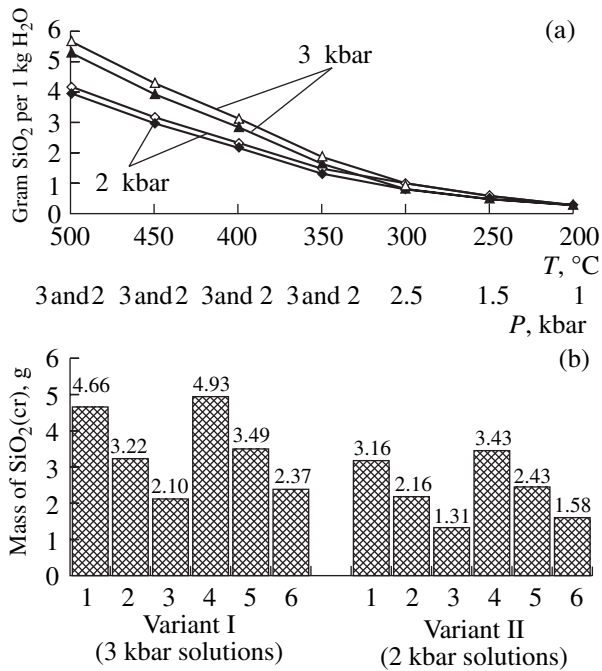


Fig. 1. Dependence of silica dissolution from unaltered granite GR14 of the lower part of the Aue cupola and its precipitation in the free space of fissures on temperature and pressure. (a) Curves of SiO_2 dissolution ($\text{g}/\text{kg H}_2\text{O}$) at pressures of 3 kbar (upper range) and 2 kbar (lower range) within temperature interval of 500–300°C, within temperature interval of 300–200°C the pressure is 2 kbar. The upper boundary of the ranges is SiO_2 solubility in pure H_2O , and the lower boundary is SiO_2 solubility in solution with $\text{Cl}/\text{CO}_2 \approx 1$; the silica solubility curves for other Cl/CO_2 ratios lie between these bounds. (b) Silica release into precipitate upon cooling of solutions from various temperatures at pressures of 3 kbar (variant I) and 2 kbar (variant II). In both variants, models 1, 2, and 3 correspond to the cooling of solutions with initial temperatures of 500, 450, and 400°C, respectively, to 350°C; models 4, 5, and 6 correspond to the cooling of the same solutions from 500, 450, and 400°C, respectively, to 300°C.

instance, if model solutions equilibrated with granite at 500°C and 3–2 kbar (i.e., at a temperature higher than that shown in Fig. 2 examples) are supplied through fractures into a cold region, they will produce a quartz richer precipitate at any Cl/C ratio, and the total content of other minerals in it will decrease to 1–3% and even lower. This fact was observed in dozens of particular models, despite the much higher (compared to 450 and 400°C) concentrations of sulfur, iron, and ore elements in the solution, and it cannot yet be explained. In contrast, the solutions equilibrated with granite under lower temperature conditions (400°C and 3–2 kbar) produced a precipitate upon cooling to 350–300°C (2.0–1.5 kbar) containing up to 20 wt % of minerals coprecipitating with quartz (mainly sulfides) (Fig. 3a), if the composition of the solution was chloride-rich. The precipitates obtained from chloride poorer solutions (formed at 400°C) (Fig. 3b) or pure water (Fig. 3c)

also contained considerable amounts of accessory vein minerals. The abundance of wolframite in these precipitates (Figs. 3a–3c) decreased compared to those produced by solutions cooled from an initial temperature of 450°C. It should be noted that the model precipitates from chloride-rich solutions shown in Figs. 2a and 3a correspond in fact to the following quartz–sulfide stage of the hydrothermal process at the Schlema deposit.

Some quantitative characteristics of the processes of silica reprecipitation and formation of quartz veins can be illustrated by the example of the precipitation of quartz and cogenetic minerals shown in Fig. 2. Let us assume that the average total mass of SiO_2 precipitated by each kilogram of solution (equilibrated with granite at 450°C and 3 kbar) is 3.3 g. Then, the formation of a small 0.5-m-thick quartz vein extending 100 m along strike and 100 m along dip (i.e., having a total volume of 5000 m^3) and containing 1.325E+04 t of quartz would require at least 4E+09 t (calculated to H_2O) of high-temperature pore solutions. There are many hundreds of such and much larger veins in the deposit. Therefore, the total mass of quartz in them and the masses of hot solutions necessary for their precipitation must have been higher by 3–4 orders of magnitude, i.e., the precipitation of E+07–E+08 t of quartz required approximately 4E+12–4E+13 t of solutions. The question is whether such a removal of SiO_2 had to change dramatically the composition of granite above the –1260 m horizon (relative to the MS level), which is taken as the lower boundary of alteration (“dispersed muscovitization”) in the upper part of the Aue cupola [17]. According to the surface map of the Erzgebirge pluton [18–20], the volume of half of the cupola beneath Schlema east of the Roter Kamm Fault (above the –1260 m horizon) is about 20 km^3 , and the mass of granite in it is more than 5E+10 t; the western part of the cupola (Gleisberg and other exposures) beneath the Schneeberg deposit is ignored. The major portion of silica and accompanying components of premineralization veins was extracted by high-temperature solutions from this part of granite (>5E+10 t). Given a silica content in the granite of 72%, the initial amount of silica in this part of the cupola had to be ~3.6E+10 t. Hence, the removal of E+07–E+08 t of SiO_2 necessary for the formation of the early quartz veins corresponds to less than one percent of the initial amount of silica in this part of the cupola. As was previously concluded [1, 17], the loss of SiO_2 from the upper part of the Aue cupola was about 1 wt % and did not cause any significant changes in the proportions of the major minerals of the granite. Consequently, the estimates of the scale of SiO_2 extraction and reprecipitation obtained from our models can be considered consistent with natural observations [14], which will be further discussed below.

In this study we did not attempt to reproduce in detail the process of formation of any particular quartz

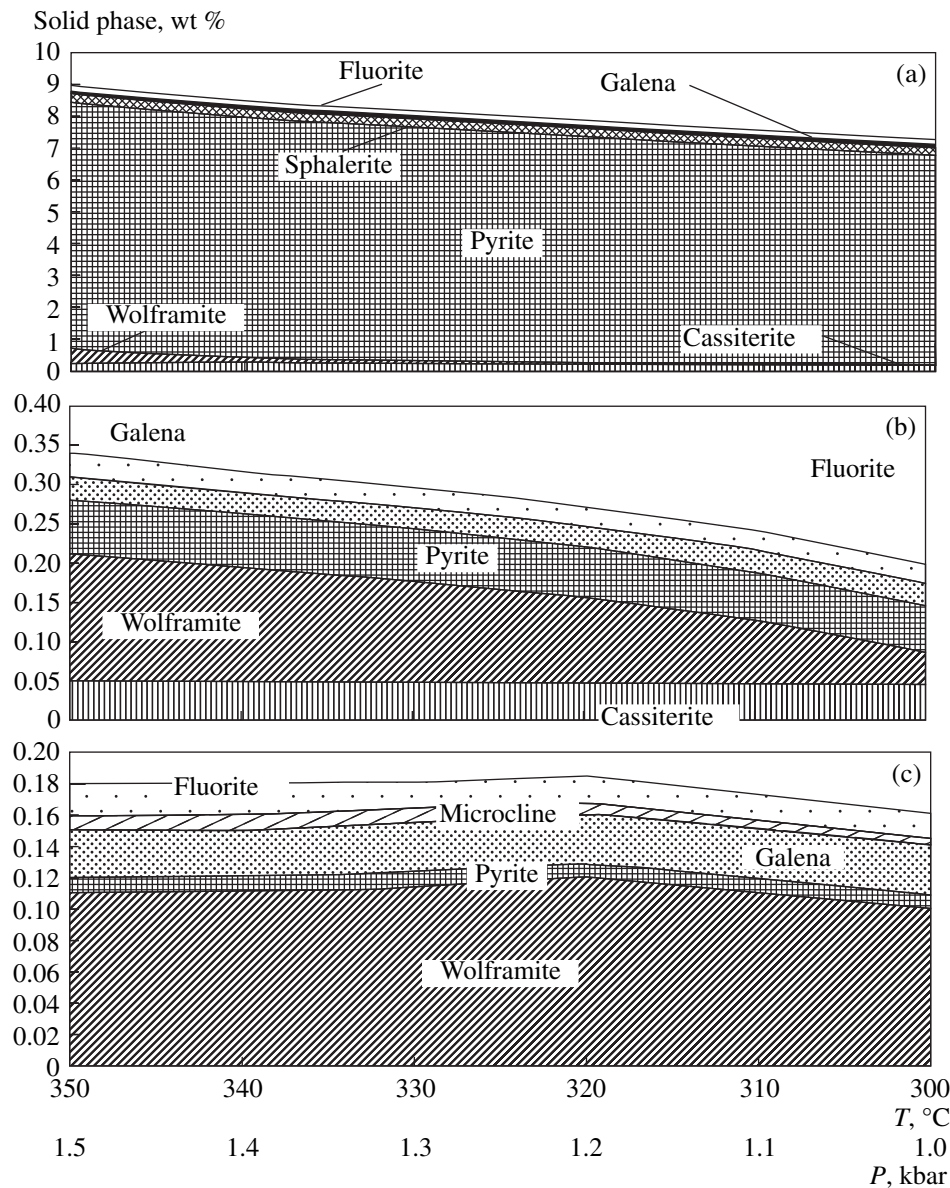


Fig. 2. Assemblages of solid phases coprecipitating with quartz from initial solutions formed at 450°C and 3 kbar during their cooling in the free space of fissures to 350–300°C and decompression to 1.5–1.0 kbar. (a) Precipitate from solution with $Cl/CO_2 \approx 11$. (b) Precipitate from solution with $Cl/CO_2 \approx 0.11$. (c) Precipitate from pure water, which was equilibrated with granite at 450°C and 3 kbar and extracted from it 0.2 mol $CO_2/kg H_2O$.

vein or a particular type of quartz veins, which show diverse proportions of quartz and fluorite, quartz and sulfides, quartz and wolframite, and various accessory phases. Therefore, we restrict ourselves to the above examples. It was important to ascertain and display three facts. *The first* is that cooling of the high-temperature (500–400°C) pore solutions from granite, the evolution of which was analyzed to some extent in part I of this study [1], can provide the formation of a precipitate identical in composition to the early quartz veins of Schlema. *The second* is that, in addition to silica, these initial pore solutions extracted from the granite and reprecipitated upon cooling tremendous amounts of

sulfur, iron, and other metals, which can be seen from Tables 1–5. *The third* is that the cooling-related precipitation of quartz and accompanying solid phases *does not require exchange reactions* between the high-temperature solutions and the environment. These tasks seem to be accomplished.

Therefore, we point out again that the results of modeling, some of which are shown here, conclusively demonstrate that *the high-temperature pore solutions infiltrating from the granite into a colder region above it (within the outlines of the ore field above the Aue cupola) could precipitate there, in the free space of fis-*

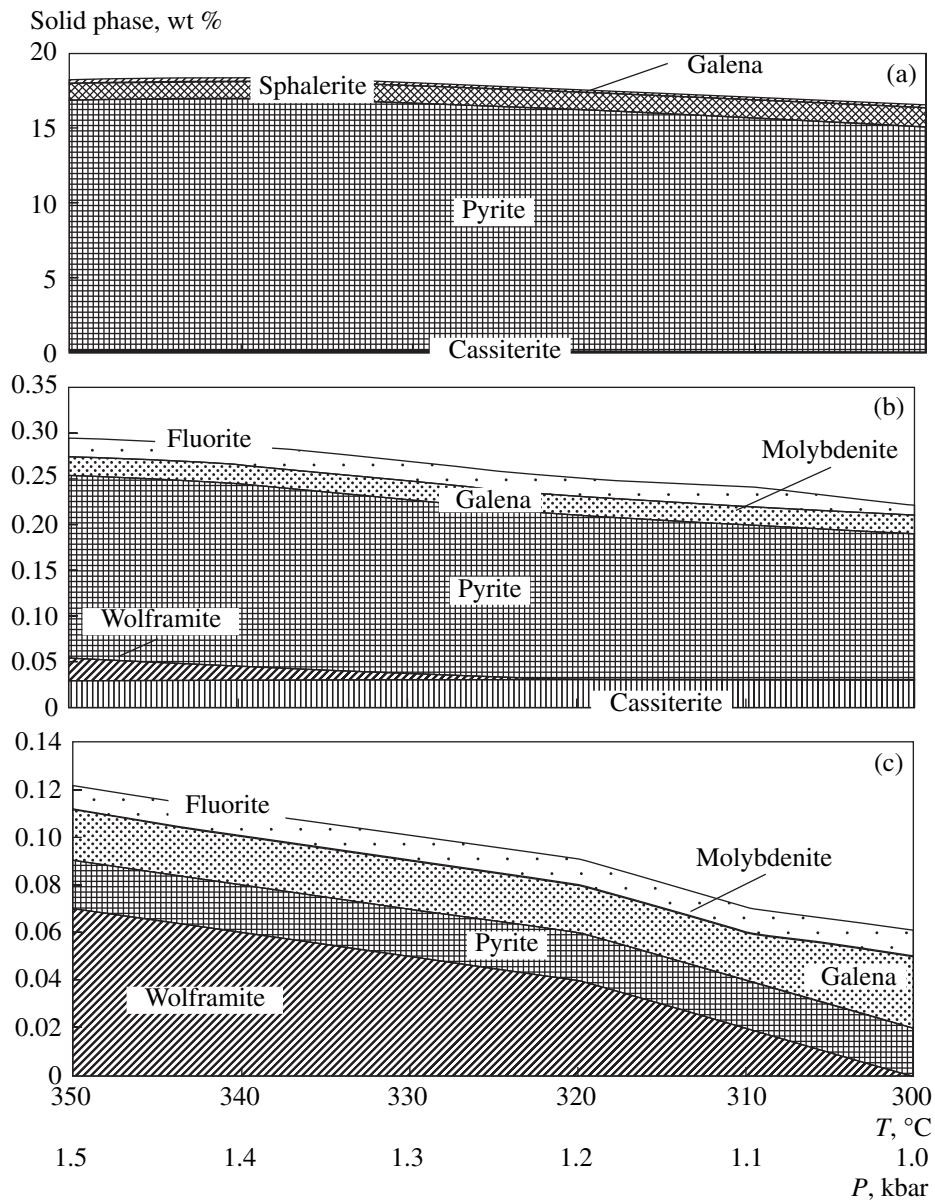


Fig. 3. Assemblages of solid phases coprecipitating with quartz from initial solutions formed at 400°C and 2 kbar during their cooling in the free space of fissures to 350–300°C and decompression to 1.5–1.0 kbar. (a) Precipitate from solution with $\text{Cl}/\text{CO}_2 \approx 11$. (b) Precipitate from solution with $\text{Cl}/\text{CO}_2 \approx 0.11$. (c) Precipitate from pure water, which was equilibrated with granite at 450°C and 3 kbar and extracted from it 0.2 mol $\text{CO}_2/\text{kg H}_2\text{O}$.

tures, material corresponding to the composition of the filling of the real quartz veins of the Schlema deposit.

QUARTZ–SULFIDE VEINS

Similar to the quartz veins, which were not the earliest quartz segregations at the deposit, the quartz–sulfide veins are also not the earliest sulfide concentrators. Pyrite and arsenopyrite bodies of various sizes and shapes developed before the beginning of formation of all fissure veins within the ore field. They were related to contact metamorphism around the Aue granite

cupola, which transformed some rocks into skarns and skarnoids. These bodies were never studied in detail at Schlema, although some data were reported by Acheev [3] and Vlasov et al. [2]. The information on quartz–sulfide bodies in the Erzgebirge was summarized by Dymkov [21]. Even the so-called sulfide horizon³ discovered beneath the southern boundary of the productive sequence at the middle and lower levels of Schlema

³ A metasomatic body, up to 3 m thick, which occurs in a skarnoid layer (presumably a former layer of carbonate-bearing rock among quartz–sericite schists) and was affected after its formation by extensive hydrothermal alterations.

was never the subject of comprehensive mineralogical and geochemical investigations. This is despite the fact that this horizon is as especially interesting as showing the highest coefficient of specific uranium ore potential among all the productive rocks of the deposit [3].⁴ In this paper, we also do not consider these sulfide bodies and draw attention to the quartz–sulfide fissure veins of Schlema predating the beginning of uranium ore formation.

Composition of Quartz–Sulfide Veins

The quartz–sulfide stage of the hydrothermal process is separated from the early quartz stage by tectonic movements and probably by a hiatus in mineral deposition. The quartz–sulfide fissure veins are usually smaller and much less abundant than the quartz veins. Acheev [3] estimated for the –810 m horizon (relative to the MS) that quartz–sulfide veins account for only 0.6% of the total thickness (i.e., volume) of fissure veins of all stages of mineralization. This means that the amount of material precipitated during the quartz–sulfide stage is about 33 times smaller than during the early quartz stage. These veins are also dominated by quartz (massive milky-white, occasionally semitransparent and drusy). The ore minerals are dominated by pyrite, arsenopyrite, chalcopyrite with bornite, sphalerite, and, to a smaller extent, galena. Pyrrhotite and troilite are less common; fahlores and arsenides were also reported, although it cannot be excluded that they were produced by the solutions of post-uranium stages affecting the sulfide veins. The quartz–sulfide veins are practically free of wolframite, but they often contain scheelite, which forms commercial concentrations at places. Hematite (specularite) occurs in rare cases in the veins and veinlets of this stage. The most common gangue minerals of the veins are fluorite, apatite, chlorites, micas, and sometimes carbonates; feldspars (adularia and albite) and other accessory phases were documented in minor amounts; sulfate (anhydrite and possibly barite) is rare. Metasomatic sulfide mineralization often develops away from the cutting, steeply-dipping veins along joints in schists, especially in carbonaceous and mafic ones; also common is the formation of abundant relatively large metacrysts of pyrite and arsenopyrite accompanied by chloritization in all the country rocks. Chloritization was also detected in the wallrocks of the cutting veins of this stage [22]. Noteworthy is the fact that the inventory of minerals of the quartz–sulfide veins (except for the replacement of wolframite by scheelite) is practically identical to that of solid phases in the early quartz veins.

The mass proportions of quartz and the bulk of ore minerals, as well as proportions of various ore phases

⁴ The coefficient of specific uranium ore potential is the ratio P_U/P_{rock} , where P_{rock} is the area of the given rock in the walls of vein fissures cutting it, and P_U is the total area of U-ore lenses in the rock.

are variable. There are rare sites and veinlets of quartz–hematite composition, quartz–massive sulfide vein segments (where pyrite and arsenopyrite are strongly dominant), and quartz–base-metal sulfide segments (quartz–sphalerite and quartz–chalcopyrite with other Cu sulfides). According to the results of fluid inclusion studies [6], these veins were formed at temperatures of 250–200°C and pressures of 1.5–1.0 kbar. If the thermal gradient remained high during their formation, the pore solutions of the granite feeding the hydrothermal system of the quartz–sulfide stage could occur at the upper levels of the Aue cupola at an initial temperature of about 400–300°C and probably higher pressure (up to 2–3 kbar).

Models of the Composition of Pore Solutions of Granite during the Formation of Quartz–Sulfide Veins

The temperature interval of quartz–sulfide vein formation is 100°C lower than that of the early quartz veins. It can be suggested that this is related to the relative cooling of rocks and pore solutions both in the ore field and in the upper part of the Aue granite cupola. The extent of cooling of granite and its pore solutions was probably also ~100°C.

The decrease in T and P in the granite–solution system by the beginning of the formation of quartz–sulfide veins resulted in significant changes (compared with 450°C) in the composition and properties of the pore solutions of granite, which were already discussed in [1, Fig. 4]. We describe here only some additional details of this change by the example of equimolar Cl/C solutions (Table 6). *First*, a decrease in temperature to 350–300°C (both at decreasing and constant P) changed the proportions of divalent elements in the model pore solution. The oxidation of iron in the granite [1] decreased the concentration of Fe in equilibrium solutions by two orders of magnitude, and the high solubility of Mn resulted in its rapid removal from the granite and complete disappearance from the solutions at $\leq 350^\circ\text{C}$. The Ca/Mg ratio changed dramatically. Owing to these changes, a new sequence of decreasing concentrations of divalent elements in pore solutions was established: $\text{Ca} \rightarrow \text{Mg} \rightarrow \text{Fe} \rightarrow (\text{Mn})$ instead of the high- T and high- P sequence $\text{Fe} \rightarrow \text{Mn} \rightarrow \text{Mg} \rightarrow \text{Ca}$. *Second*, the bulk concentration of sulfur in the solution decreased by an order of magnitude, and the concentration of sulfide sulfur decreased even more dramatically.⁵ *Third*, the bulk concentrations of metals and speciation of all components, both ore and rock-forming, changed in the pore solutions [1, Figs. 5, 8].

⁵ At 500–400°C, S(II) accounts for more than 90% of the total dissolved sulfur; at 350°C, simultaneously with the decrease in the bulk concentration of sulfur, the fraction of S(II) decreased by a factor of almost two; and at b and below, S(II) accounts for less than 2% of the bulk concentration of remaining sulfur. Hence, the concentration of S(II) in the pore solutions decreased by more than three orders of magnitude by 300°C, and these solutions contained practically only sulfate sulfur.

Table 6. Variations in the composition of pore solutions from granite with equal molar concentrations of MCl and H₂CO₃ at various *T* and *P*

Element	<i>T</i> , °C			
	400	400	350	300
	<i>P</i> , kbar			
	3	2	2.5	2
H	2.416E+00	2.379E+00	2.301E+00	2.229E+00
O	1.565E+00	3.520E+00	3.432E+00	3.382E+00
K	2.110E-01	2.178E-01	1.737E-01	1.324E-01
Na	9.534E-01	9.331E-01	9.567E-01	1.019E+00
Ca	4.623E-05	4.497E-05	7.336E-05	1.475E-04
Mg	5.701E-05	7.996E-05	3.444E-05	5.108E-05
Mn	1.254E-04	1.994E-04	0	0
Fe	1.246E-03	2.130E-03	1.698E-05	1.237E-05
Al	1.993E-06	5.175E-06	7.775E-07	2.915E-07
Ti	3.769E-06	5.843E-06	6.647E-06	1.171E-05
Si	4.723E-02	3.600E-02	2.884E-02	1.679E-02
Cl	1.111E+00	1.111E+00	1.098E+00	1.103E+00
F	1.668E-02	1.172E-02	5.736E-03	3.626E-03
S	3.011E-02	3.107E-02	8.834E-03	1.404E-03
C	1.102E+00	1.101E+00	1.098E+00	1.103E+00
P	1.199E-06	4.157E-07	1.187E-06	3.436E-07
W	9.634E-06	4.134E-06	1.394E-06	4.095E-07
Sn	3.606E-05	1.591E-05	2.112E-08	2.164E-09
Mo	9.134E-10	3.952E-10	2.318E-10	6.267E-07
Pb	1.240E-05	1.786E-05	5.085E-06	1.391E-04
Zn	6.960E-05	3.072E-04	3.702E-05	1.234E-03
Cu	9.851E-07	4.188E-07	1.861E-07	5.075E-08
U	6.836E-11	2.246E-10	1.023E-10	7.723E-11
I	0.796	0.73	0.856	0.942
pH	5.348	5.298	5.403	5.475
Eh, mV	-624	-600	-565	-481

Fourth, Table 6 illustrates an interesting phenomenon, which we previously proposed [1] to call the Borisov–Shvarov effect, of a sharp increase (by two orders of magnitude and more) in base metal concentrations in the pore solutions of granite at a certain step of interaction at the expense of gradually accumulated changes in the granite–solution system (cf. Tables 1–5 and the last column in Table 6). Thus, the modeling of processes occurring at the *T* and *P* of quartz–sulfide vein formation should account for the fact that the pore solutions of granite participating in these processes were signifi-

cantly different from the solutions of higher temperature stages.

Models of Formation of Quartz–Sulfide Precipitates

Since the material precipitated in the quartz–sulfide veins is dominated by quartz, it is evident that the main result of the hydrothermal process was also the transportation of silica and its precipitation owing to the cooling of the silica-bearing solutions. In fact, quartz–sulfide precipitates similar to the *average composition* of the quartz–sulfide veins were obtained in models during the simulation of the formation of quartz veins (Figs. 2a and 3a). In addition to the identity of mineral associations of the quartz–sulfide and quartz veins, this allows us to consider the quartz–sulfide veins as a sort of small final chord (probably, 1/33) of the major premineralization process of SiO₂ (and the same set of accompanying components) redeposition by thermal solutions from the Aue granite cupola into the ore field.

However, if the pore solutions feeding the fissure systems of the quartz–sulfide stage were equilibrated with granite at 350–300°C, their cooling does not produce a model precipitate exactly reproducing the average composition of the quartz–sulfide veins. As can be seen from Fig. 4, the solutions equilibrated with the Aue granite at 350°C and 2.5 kbar (Table 6) can precipitate quartz (1.18–1.45 g SiO₂ per 1 kg H₂O) upon cooling to 250–200°C (with a *P* decrease to 1.5–1.0 kbar). However, the production of ore minerals is rather minor in this case: only 0.45 wt % of sphalerite, pyrite, and galena, plus chalcopyrite (replaced by bornite at 220°C), molybdenite, scheelite, cassiterite, U(TiO₄)₂, fluorite, F-apatite, epidote, and muscovite. The solution shown in column 4 of Table 6 equilibrated with granite at lower temperature (300°C and 2 kbar) precipitates even 50% less quartz, 0.46–0.73 g/kg H₂O, at the same decrease in *T* and *P*; whereas sulfides are absent in the assemblage, and the precipitate has a quartz–hematite composition (Fig. 4b) similar to the quartz–hematite material that predated in the Erzgebirge the deposition of the major portion of sulfides in the veins and veinlets of this stage [20]. The other minerals of this model are fluorite, F-apatite, Mg-chlorite, muscovite replaced by kaolinite at 200°C, and traces of scheelite, cassiterite, and the same U titanate. The reasons for such dramatic depletion of model precipitates in sulfides were discussed in [1] and in this paper during the analysis of Table 6. A decrease in the concentration of Fe in solutions equilibrated with granite at 350–300°C by two orders of magnitude compared with the pore solutions obtained at 450–400°C, a factor of two decrease of Pb and Zn concentrations by 350°C, and, most importantly, the considerable deficit of sulfide sulfur predetermined the low threshold of possible sulfide formation. Even a new increase in the concentration of base metals by almost two orders of magnitude by 300°C (compared to 350 and even 400°C) related to the Borisov–Shvarov effect [1] do not improve the model

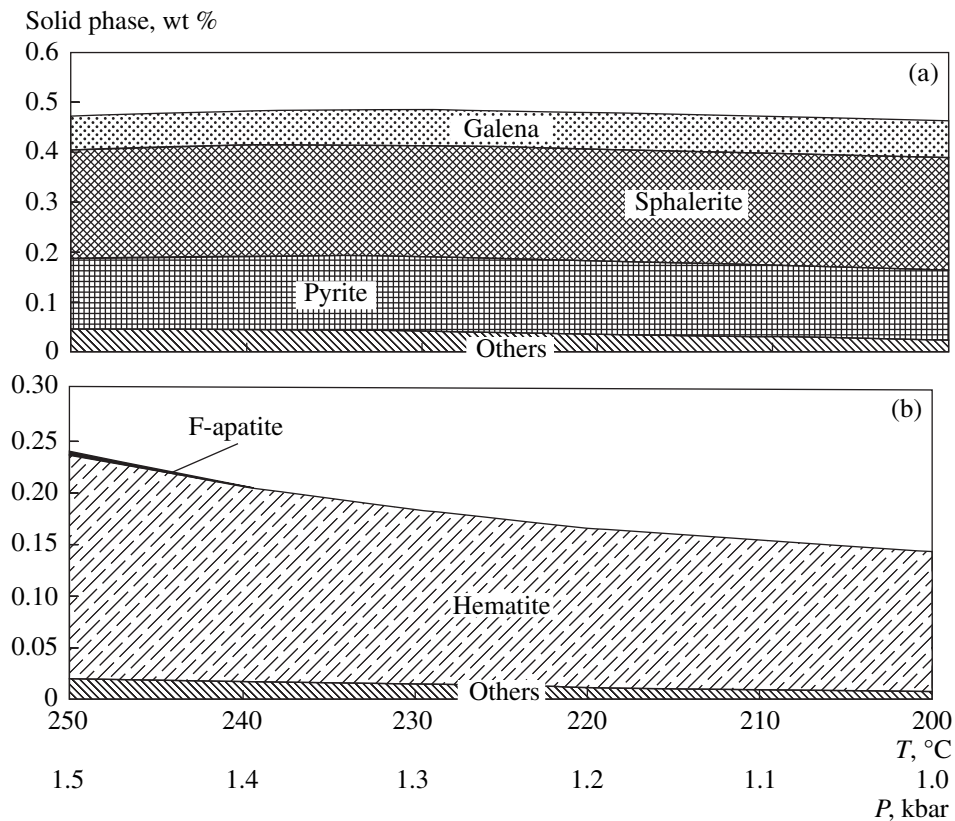


Fig. 4. Assemblages of solid phases coprecipitating with quartz from initial solutions formed at 350–300°C (Table 6) during their cooling in the free space of fissures to 250–200°C and decompression to 1.5–1.0 kbar. (a) Precipitate from solution with initial $T = 350^\circ\text{C}$, $P = 2.5$ kbar, and $\text{Cl}/\text{CO}_2 \approx 1$. (b) Precipitate from solution with initial $T = 300^\circ\text{C}$, $P = 2$ kbar, and $\text{Cl}/\text{CO}_2 \approx 1$.

situation, because there is no S(II). The concentration of H_2S in equilibrium with the quartz–hematite precipitate (Fig. 4b) decreased in the model to a figurative value of $E-69$ mol. The high total concentrations of base metals in the solution ($\sim 1.5E-03$ mol, which is higher than in the pore solutions obtained at 500–400°C) could potentially provide ~ 15 – 20% of sulfides in the precipitate (for the aforementioned quartz release). However, the absence of S(II) necessary for their precipitation retains all the base metals and, especially, iron in the aqueous phase.

What could promote the precipitation of Zn–Cu–Pb sulfides, which are widespread in the real veins of this stage? The reason was obviously the input of sulfide sulfur from an external source into the metal-bearing solutions directly in the zone of vein formation of this stage. And this is not an utopia. Already Betekhtin [23] noted the “the reason for the extensive generation of ore minerals is the contact of ascending hydrothermal solutions with solutions of a different composition.” A similar statement was made by Smirnov [24]: “Probably much more frequently [compared with the interaction of the components of a single solution or solution and environment, which was discussed above, VB, exchange reactions occur as a result of mixing of hydro-

thermal solutions ... entering from depths with ground waters of various levels of circulation.” The same idea was even more explicitly expressed by Skinner [25, p. 25], who argued that the common reasons for ore formation are probably chemical processes occurring during mixing of two solutions of different compositions, a precipitating component, for example H_2S , can be introduced during mixing into the metalliferous solution. Pek and his colleagues [26–29] used hydrodynamic models to show the inevitable entrainment into fissure channels of pore solutions from rocks and their mixing in the fissures. The conditions at Schlema, including the multiple intersections of variably permeable rocks by subvertical fractures, were favorable for such an ore formation mechanism by the mixing in fissures of H_2S -free metalliferous solutions of the late quartz–sulfide stage with pore solutions entrained from the productive rocks enriched in hydrogen sulfide [30]. We showed above that such mixing could be subsequently the main reason for the precipitation of uranium in the fissure veins of the next stage of mineral formation. Similar considerations apply to base metal sulfides. In a series of special models, we evaluated the consequences of this probable paleohydrodynamic event, mixing of metal-bearing solutions 3 and 4 (Table 6) with the pore solutions from the productive and nonproduc-

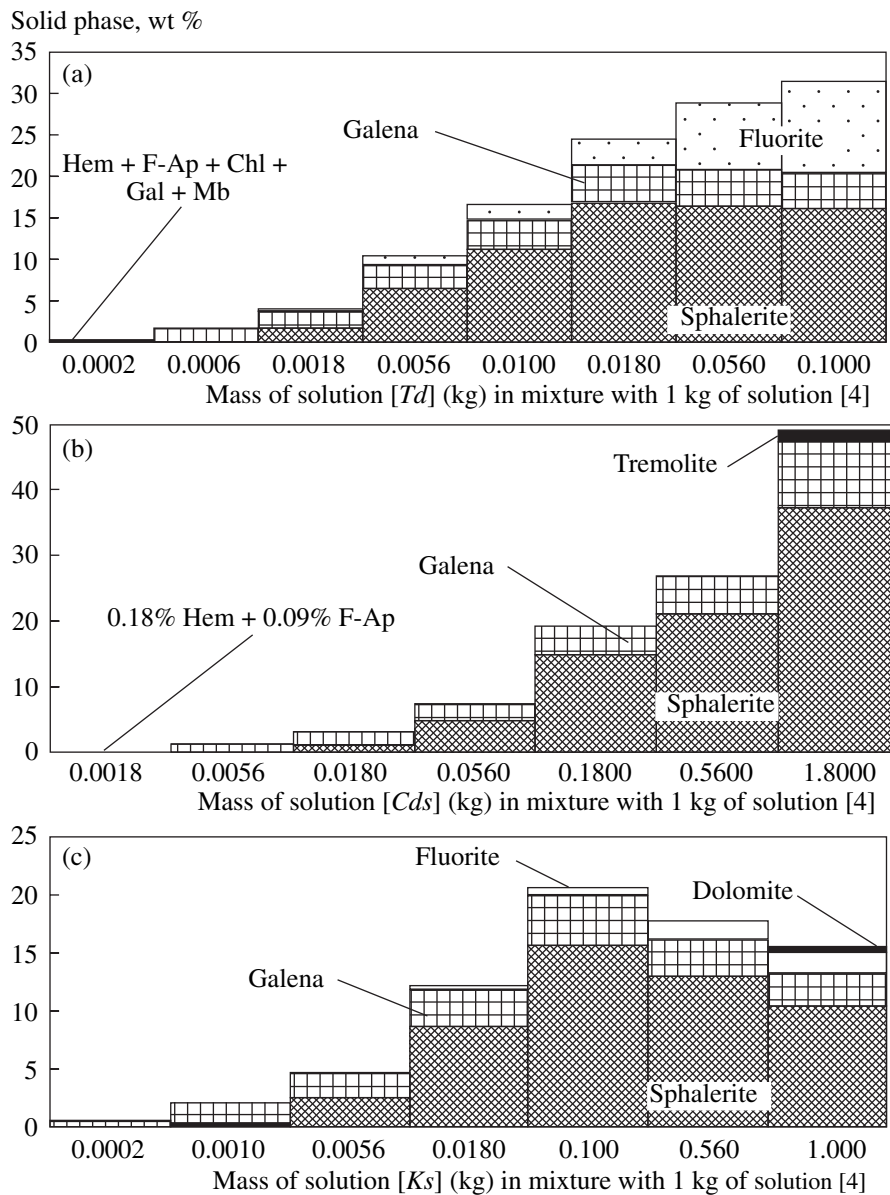


Fig. 5. Assemblages of solid phases coprecipitating with quartz during mixing in the free space of fissures of a solution with initial $T = 300^{\circ}\text{C}$, $P = 2$ kbar, and $\text{Cl}/\text{CO}_2 \approx 1$ (Table 6) and pore solutions from the productive sequence of Schlema: (a) pore solutions from banded amphibole schists (Td), (b) pore solutions from dark phyllites (Cds), and (c) pore solutions from carbonaceous schists (Ks).

tive rocks of Schlema. These results are shown in Fig. 5. The models reproduced mixing of 1 kg H_2O of solution 4 (Table 6), which yielded a hematite–quartz precipitate upon cooling, with gradually increasing masses of pore solutions from the rocks of the deposit; the amounts of the latter in fractions of a kilogram are shown along the x axis. These models are exemplified by pore solutions from the main productive rocks of Schlema: banded amphibole schists Td, dark phyllites Cds, and carbonaceous schists Ks [30, series C]. As can be seen from Fig. 5, the addition of only 0.1–1.0 g of pore solutions from the productive country rocks of Schlema to one kilogram of solution 4 is sufficient to provide a change from the hematite–quartz precipitate

to a sulfide–quartz one. As the fraction of the pore solutions in the mixture with the ore-bearing solutions increases, the content of base metal sulfides in the precipitate rises up to 20 wt % and higher, and other phases coprecipitate with quartz and sulfides, including fluorite, tremolite (or Mg-chlorite), carbonates (dolomite in Fig. 5b and calcite in other models), and a number of other accessory phases, which occur in natural veins. The pore solutions of some nonproductive rocks (hosting very low amounts of vein-type U ores) can also precipitate sulfides and other minerals cogenetic with quartz by mixing with the ascending solutions of the same composition (Fig. 6a). At a very high fraction of these solutions in the mixture with solution 4, sulfate

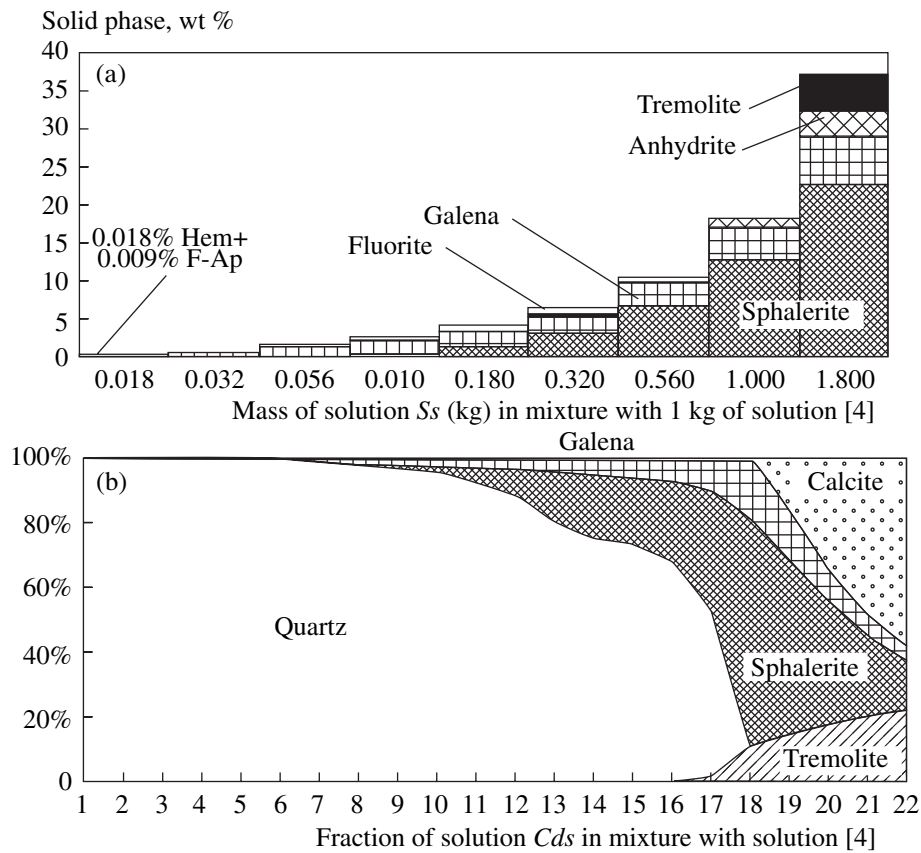


Fig. 6. Assemblages of solid phases coprecipitating with quartz during mixing of a solution with initial $T = 300^{\circ}\text{C}$, $P = 2$ kbar, and $\text{Cl}/\text{CO}_2 \approx 1$ (Table 6) and pore solutions from the rocks of Schlema: (a) with pore solutions from light-colored quartz-sericite schists (S_s), (b) with pore solutions from dark phyllites (C_d s) corresponding to the continuation of Fig. 4b to the right (it was truncated at step no. 17), i.e., at an increase in the fraction of this pore solution in the mixture up to 56/1.

may occur in the precipitate. It is represented by anhydrite in our models, but the appearance of barite is also possible, if Ba is available in the system. If paleohydrodynamic conditions were such at some sites that the mixed solutions contained relatively little ore-bearing solutions and were strongly dominated by pore solutions, for instance, from dark phyllites C_d s, the models suggest the possible formation of a quartz-free precipitate (83% sphalerite + 18% galena + 9% tremolite or Fe-Mg chlorite in other models), which is rather common in the segments of veins of this stage with abundant sphalerite, galena, and chalcopyrite-bornite, and, then, a sulfide-tremolite (chlorite)-calcite precipitate (Fig. 6b).

In general, this rather common in natural environments mixing of *low-temperature sulfur-free* granite-derived solutions with the pore solutions of the enclosing rocks of Schlema could provide extensive deposition of chalcophile element sulfides in veins: sphalerite, galena, chalcopyrite, and other Cu sulfides. However, it could not initiate the precipitation of pyrite and arsenopyrite, whereas these Fe *chalcogenides* are in general predominant among the ore minerals of the quartz-sulfide veins of Schlema. The concentration of Fe in the

low-temperature granite-derived solutions is one-to-two orders of magnitude lower than the concentrations of Zn, Pb, and Cu. Moreover, the pK of pyrite-forming reactions at $250\text{--}200^{\circ}\text{C}$ and 1 kbar (19.32–19.81) is about two orders of magnitude lower than the pK of formation of sphalerite and galena under the same conditions (about 21–22) and much lower than the pK of formation of Cu sulfides (~ 49 for chalcopyrite). Thus, iron has no chance to compete with chalcophile metals for sulfide sulfur, independent of its source in the vein fissures.

The precipitation of Fe *chalcogenides* can be related to the inflow into the vein fissures of hotter S(II)- and Fe(II)-rich solutions, for instance, those equilibrated with granite at 400°C and 3–2 kbar (Tables 1, 6). Indeed, their cooling to the T P conditions of the quartz-sulfide stage produces a material containing tens of weight percent Fe sulfides. Such model precipitates are illustrated in Fig. 7. Figures 7a and 7b show sequential changes in the composition of precipitates from such pore solutions. The first model precipitate (Fig. 7a) was obtained at the expense of cooling of these solutions to $250\text{--}200^{\circ}\text{C}$, while pressure dropped to 1 kbar and remained constant over the whole T inter-

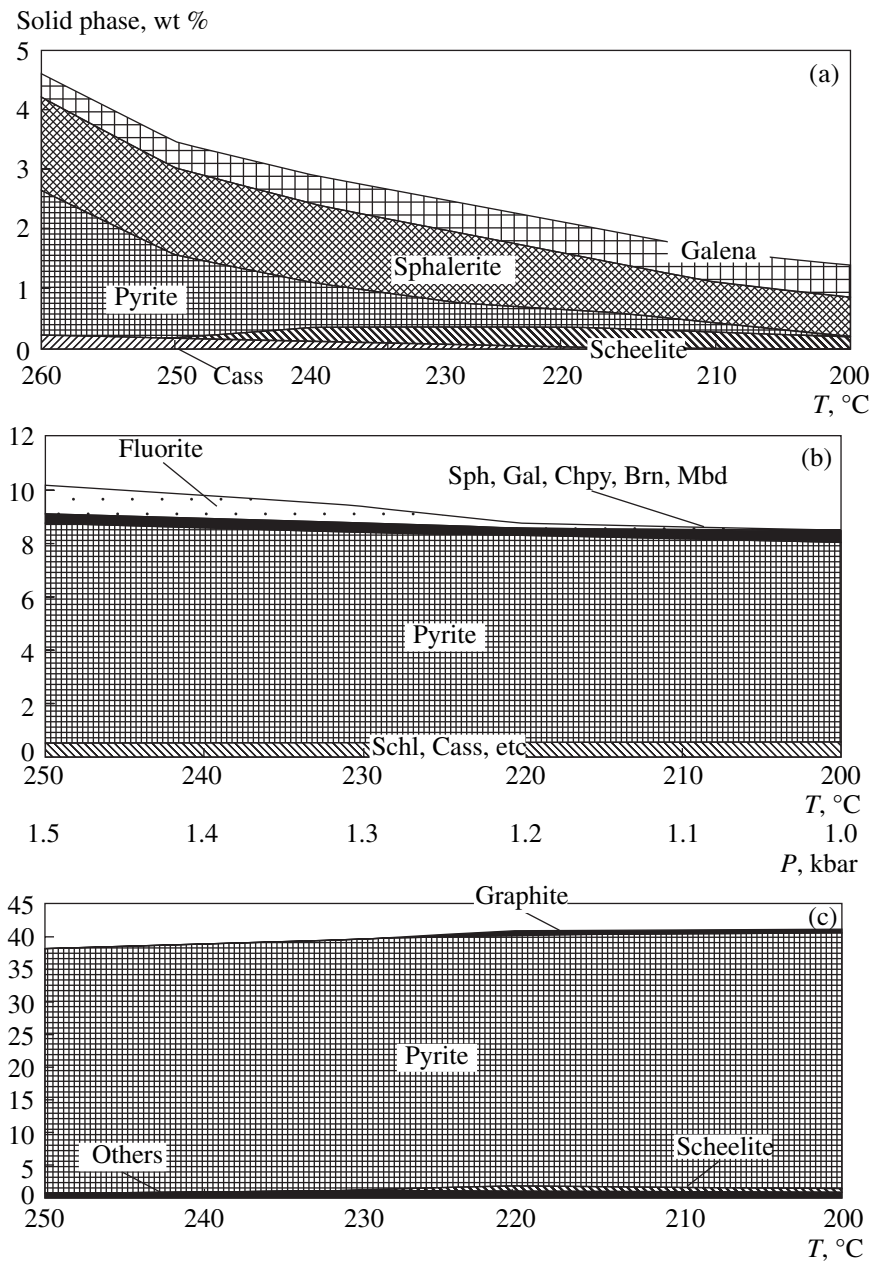


Fig. 7. Assemblages of solid phases coprecipitating with quartz from initial solutions formed at 400 °C and 2 kbar during their cooling in the free space of fissures to the temperatures of the quartz–sulfide stage of the hydrothermal process (260–200 °C) and decompression to 1.5–1.0 kbar. (a) Cooling of initial solution with Cl/CO₂ ≈ 1 to 260–200 °C and decompression to a pressure of 1 kbar, which remained constant within the entire temperature interval. (b) Cooling of initial solution with Cl/CO₂ ≈ 11 to 250–200 °C accompanied by a stepwise pressure decrease to 1.5–1.0 kbar within this temperature interval. (c) Cooling and decompression of a more mineralized initial solution containing 3 mol NaCl + 2 mol H₂CO₃ from 400 °C and 2 kbar to 250–200 °C and 1 kbar; the pressure remained constant within the whole temperature interval.

val. The second precipitate (Fig. 7b) was obtained at the expense of a simultaneous decrease in both temperature and pressure in the same *T* interval. Figure 7c shows that the cooling and decompression of a more mineralized solution (3 mole MCl + 2 mole H₂CO₃) also equilibrated with the granite at 400 °C and 2 kbar can result in the precipitation of ~60 wt % quartz and ~40 wt % pyrite. We do not discuss here the real existence of such

solutions at Schlemma, but this model illustrates how an increase in mineralization may affect the intensity of Fe(II) and S(II) transportation and release of sulfides into the precipitate during cooling of such solutions.

It is conceivable that the composition of the real quartz–sulfide veins of Schlemma could (or should?) be formed under the influence of a series of different solutions precipitating their loading owing to different fac-

tors. The following logical sequence of events can be imagined. Fissures opened at the beginning of the quartz–sulfide stage (after a short hiatus in solution infiltration) were fed for a short time by already relatively cold (350–300°C) iron- and sulfur-poor solutions from the apical zone of the Aue cupola. Owing to a decrease in T and P , they could produce small amounts of quartz and hematite–quartz precipitates similar to those shown in Fig. 4. As pore solutions from deeper and hotter parts of the cupola with high S(II) and Fe concentrations were extracted into the vein fissures, their cooling to 250–200°C could be responsible for the precipitation of the major portion of Fe sulfides in these veins. A new episode of weakening of solution infiltration terminating this stage resulted in a decrease in the initial T and P values of solutions in the granites of the Aue cupola. During cooling outside the cupola, these solutions (enriched in Zn, Pb, and Cu but depleted in sulfide sulfur) could precipitate the main portion of base-metal sulfides in the fissures, but only at the expense of their mixing with H₂S-bearing pore solutions from the country rocks of Schlema.

Other scenarios can be proposed for changes in the assemblages of real quartz–sulfide veins. Of particular importance is the principal essence of the phenomena, that is, in any case *the pore solutions of the granites of the Aue cupola could provide the formation of all assemblages from the real quartz–sulfide veins in cutting fractures at the expense of both their cooling in fissures among the rocks of the ore field and reaction with these rocks (pore solutions are an inherent part of rocks) accompanying their cooling.*

It is possible that the mixing of granite-related solutions with the pore solutions of the ore-hosting rocks of Schlema resulting in the models in the appearance of Fe–Mg chlorite and other Fe–Mg silicate phases in the precipitate, which can be seen in Figs. 5 and 6, could be responsible for the chloritization of the country rocks near the quartz–sulfide veins [22]. However, further modeling and analysis are needed to address this problem.

ROLE OF PREMINERALIZATION VEINS FOR SUBSEQUENT URANIUM ACCUMULATION

Using thermodynamic models, we analyzed only the general tendencies of processes occurring at Schlema in the premineralization period. Nonetheless, their analysis allows us to address the most interesting problems: why the uranium ores of Schlema, as well as in the majority of other vein-type uranium deposits, were formed only after the extensive redeposition of silica and accompanying components, mainly sulfides, from granite into the overlying fissure systems of the deposits. What were these early high-temperature processes important for the subsequent uranium transportation from the granite and its concentration in fissure veins? Would U ore veins have appeared at Schlema, if the hydrothermal process had occurred there only at 200°C, and the uranium stage had been the earli-

est? These questions are probably interesting for many researchers.

We calculated above that the extraction from granite and deposition in fissures of E+07–E+08 t of silica, i.e., the estimated amount of silica in the early quartz veins of Schlema, required 4E+12 to 4E+13 t of solution. This is close to the real situation (see below) and is not surprising. However, the fact that the same volume of high-temperature solution equilibrated with the granite *extracted (and could not help extracting!) from the granite a considerable molar amount of sulfur, approximately equal (Tables 1, 2) or even higher (Table 3) than that of silica* is not trivial. The mass of extracted sulfur is only half that of silica (molecular weight of S is almost two times lower than that of SiO₂). This implies that during the early quartz stage of the hydrothermal process, 5E+06 to 5E+07 t of sulfur was removed from the upper part of the Aue cupola, although the initial content of sulfur in the same volume of granite (its concentration is 0.04–0.02 wt %) was almost 2000 times smaller than that of SiO₂. Such a loss of bulk sulfur was accompanied by progressive oxidation of the remaining S(II) in the granite to sulfate and, consequently, a much more extensive (by several orders of magnitude) decrease in the concentration of sulfide sulfur in the rock.

The same applies to iron. The molar and mass amounts of ferrous iron extracted by high-temperature solutions from the granite during the quartz stage were only an order of magnitude lower than those of silica, i.e., at least E+06–E+07 t. The remaining amount of ferrous iron in the rock was rapidly oxidized owing to interaction with the water phase (Fe oxidation factor in the granite increased from <5% in the lower half of the Aue cupola to 30–70% in its apical zones [1, 17, 18]).

In addition, high-temperature pore solutions dissolved all carbon from the granite, part of which could be present in an elementary form [28] and also contributed to lowering the Eh values of the system, and reprecipitated it in the granite as accessory carbonates in response to a temperature decrease.

This extensive removal of reducing agents from the granite in the premineralization period has escaped the attention of researchers, although it has been reliably documented by petrographic and analytical observations at least since 1996 [1, 17, 18]. Owing to this phenomenon, the redox conditions of the granite–solution system changed dramatically *after the pre-uranium stages* of the hydrothermal process *as a result of its physicochemical “work.”* This work resulted not only in apparent changes (formation of early quartz and quartz–sulfide veins of the deposit) but also in a superficially imperceptible sharp increase in the potential extensive release of uranium from the granite (where it remained almost immobile yielding E–11 to E–10 mol in the water phase) into solutions infiltrating through the Aue cupola *after the premineralization stages* of the hydrothermal process.

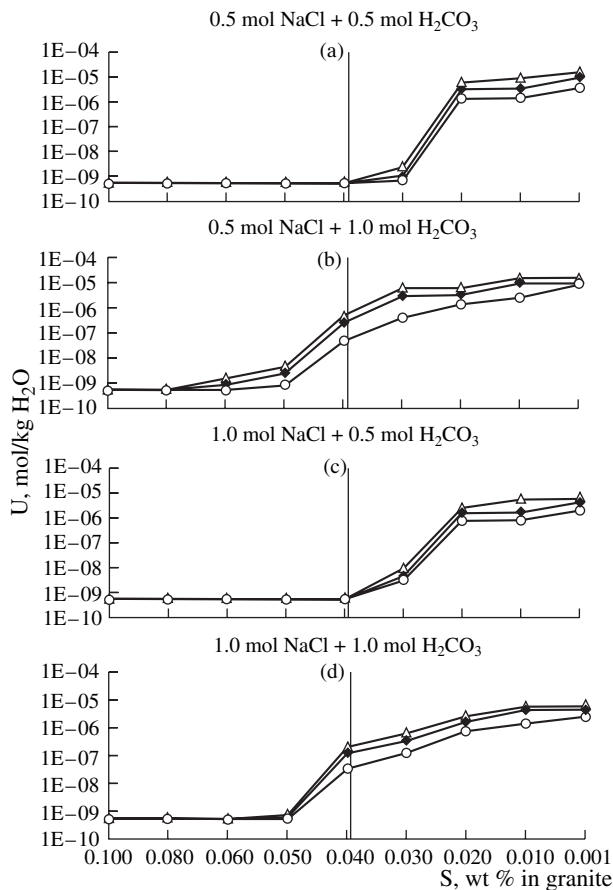


Fig. 8. Uranium release from a granite with background uranium content [31] into solutions of variable composition at temperatures of 250, 200, and 150°C and a pressure of 1 kbar as a function of bulk sulfur content in the solid phase of the granite. Diagrams (a)–(d) correspond to various proportions of NaCl and H₂CO₃ in the solution affecting the granite.

In order to support this conclusion, let us consider using special models such as the influence of changes in the *content of a single component (sulfur or carbon)* in the granite on the behavior of uranium in the granite–solution system and extraction of U from the rock by the solutions. Since this issue concerns not only our granites, we disregard for the moment the problems of Schlema and, instead of the concrete Aue granite (which shows, in particular, an unusually high background U content), use the classical average composition of granite after Zavaritskii [31], which was previously investigated by us [32–34]. A constant amount of uranium was introduced into this granite. This amount corresponded to the average uranium abundance in felsic rocks (3.5E–04% after Vinogradov [35]) rather than the high content of the Aue granite [17, 18]. Changing sequentially *only sulfur content* in the granite, we modeled its interaction with carbon dioxide–chloride aqueous solutions up to the attainment of thermodynamic equilibrium in the granite–solution system. It should be taken into account that the redox potential of the system

is almost independent of the initial form of sulfur in the granite (FeS, FeS₂, S⁰, SO₂, or SO₃) [29]; in our models it was introduced as S⁰. Calculations were carried out for the temperatures of uranium ore formation, 250, 200, and 150°C and a pressure of 1 kbar. The mass of solution (with variable molar proportions and bulk concentrations of NaCl and H₂CO₃) was taken to be $W = 1$ kg H₂O, and the mass of granite (R) was 10 kg (it was noted above that the mass ratio $R/W = 10$ provides the attainment of equilibrium in the granite–solution system). The results of 270 particular models are summarized in Fig. 8. Curves corresponding to various temperatures are denoted by symbols: unfilled triangles for 150°C, filled diamonds for 200°C, and unfilled circles for 250°C. As follows from the simulation and illustrated by examples in Fig. 8, the intensity of uranium release from the granite *providing its ore concentrations ($\geq 10^{-6}$ mol)* in the solutions equilibrated with the granite is attained in two cases: (1) when the bulk content of sulfur in the initial granite is 1.5–2.0 times lower than its average abundance after Vinogradov (shown by the vertical line in the diagrams), and (2) if the initial high (average granitic abundance or higher) sulfur content in granite was decreased to a level 1.5–2.0 times lower than the background value by some preliminary processes. The level 0.2 wt % S, below which considerable (ore) amounts of uranium are extracted into the aqueous solution, is, of course, not constant and can be shifted to the right or to the left in Fig. 8 owing to variations in the compositions of interacting granite and solution. For instance, ore concentrations of uranium were obtained in Fig. 8b in a CO₂-dominated solution at a bulk sulfur content of 0.03 wt %. However, there is always such a threshold sulfur content in the solid phase separating the conditions of existence of uranium-bearing and uranium-free equilibrium solutions.

Let us consider this threshold in more detail. Of course, it is expressed not only in sulfur content, although changes in the granite–solution system are tabulated against this variable. It was previously shown that changes in the content of any element in the rock, including variable-valence elements, causes reequilibration and changes in the proportions of all solid phases, even those not containing this particular element. The same applies to the species of solution in equilibrium with the rock [32–34]. The situation in the present models is identical: under any conditions (T , P , and Cl/CO_2), the same initial solution reacts with the same granite, and *only different bulk contents of a minor component, sulfur, are specified*. However, a change in the bulk content of S causes a number of accompanying disturbances in the granite–solution system. The models reveal changes in the proportions of almost all solid phases in the rock and species in the solution, related to the thermodynamic equilibration between them at any preset S content in the granite (Table 7). A decrease in S content causes a slight increase in the contents of quartz, microcline (at 250°C and low S contents, part of K is fixed in phlogopite, which prevents an increase in K feldspar content),

Table 7. Reactions between granites with different sulfur contents and aqueous solutions containing 1.0 mol NaCl + 1.0 mol H₂CO₃ at 150 and 250°C and 1 kbar

150°C					250°C				
S, wt %	0.1	0.04	0.02	0.001	S, wt %	0.1	0.04	0.02	0.001
Quartz	30.16%	30.61%	30.66%	30.62%	Quartz	30.22%	30.08%	30.39%	30.91%
Hematite	0	0	0	0.23%	Hematite	0	0	0	0.09%
Muscovite	5.91%	5.89%	4.14%	4.14%	Muscovite	5.96%	5.53%	4.95%	4.50%
Microcline	19.82%	19.87%	21.09%	21.09%	Phlogopite	0	0	0.73%	2.28%
Albite	31.96%	31.20%	31.47%	31.75%	Microcline	19.61%	19.96%	19.90%	19.22%
Epidote	2.33%	3.74%	5.54%	5.83%	Albite	31.96%	31.87%	31.75%	31.98%
Tremolite	2.84%	2.47%	0.48%	0	Epidote	2.56%	3.75%	5.56%	6.73%
Fe-chlorite	5.68%	5.30%	4.66%	4.05%	Tremolite	2.84%	2.85%	1.72%	0
Mg-chlorite	0	0	1.09%	1.42%	Fe-chlorite	5.60%	5.30%	4.67%	4.07%
Calcite	0.99%	0.50%	0	0	Calcite	0.94%	0.54%	0	0
Dolomite	0	0.43%	0.88%	0.88%	Dolomite	0	0	0.31%	0.21%
Pyrite	0.07%	0	0	0	Pyrite	0.07%	0	0	0
Anhydrite	0.25%	0	0	0	Anhydrite	0.25%	0.14%	0.01%	0
UO ₂	0.00%	0.00%	0	0	UO ₂ (cr)	0.00%	0.00%	0	0
U ₄ O ₉ (cr)	0	0	0.00%	0.00%	U ₄ O ₉ (cr)	0	0	0.00%	0
					U ₃ O ₈ (cr)	0	0	0	0.00%
I	1.12	1.287	1.177	1.069	I	0.955	0.996	1.048	0.968
pH	6.23	6.133	6.162	6.193	pH	5.542	5.524	5.509	5.533
Eh, mV	-364	-118	-74	-64	Eh, mV	-447	-255	-177	-153
U(mol)	5.86E-10	2.04E-07	2.51E-06	5.96E-06	U (mol)	5.02E-10	3.35E-08	1.30E-06	4.44E-06
UO ₂ (aq)	5.86E-10	5.89E-10	3.32E-10	2.77E-10	UO ₂ (aq)	5.02E-10	5.06E-10	3.34E-10	2.48E-10
UO ₂ (CO ₃) ₂	6.75E-16	1.43E-7	1.66E-06	3.82E-06	UO ₂ (CO ₃) ₂	1.07E-13	3.11E-08	1.25E-06	4.30E-06
UO ₂ (CO ₃) ₃	1.32E-17	5.60E-08	8.03E-07	2.06E-06	UO ₂ (CO ₃) ₃	6.20E-17	1.46E-10	8.56E-09	3.36E-08

Mg-chlorite (phlogopite is formed instead of chlorite at 250°C), and epidote in the granite. The amount of albite does not change significantly. The contents of muscovite, tremolite, and Fe chlorite decrease. Calcite either disappears or is replaced by dolomite; pyrite and anhydrite disappear; and hematite appears. Although seemingly slight, these changes in the mineral composition of granite are accompanied by changes in the bulk composition of equilibrium solutions. The depletion of S in the granite changes the ionic strength of solutions, slightly decreases pH, and increases Eh by almost 300 mV. The combination of *all these minor changes* exerts a dramatic influence on the behavior of uranium. As can be seen from Table 7, a decrease in the amount of sulfur results in the replacement of the low-soluble solid uranium phases of the granite (uraninite UO₂(cr) and U(IV) titanates) by thermodynamically stable under new conditions and much more soluble phases, U₄O₉(cr) and even U₃O₈(cr). Simultaneously,

the former U solution species, UO₂(aq) and other U(IV) ions, are changed by uranyl carbonate ions, UO₂(CO₃)₂²⁻, UO₂(CO₃)₃⁴⁻, and others. These changes cause an abrupt increases in the bulk concentration of uranium in the solutions by more than four orders of magnitude (which is also a manifestation of the Borisov–Shvarov effect [1], an increase in the solubility of some components at the expense of accumulated changes in other components), and the solutions become uranium-bearing and ore-forming. Of course, these calculations are concerned with the *thermodynamic equilibria* toward which natural systems of the same composition tend but which are not always attained in nature because of kinetic limitations. However, the complete transformation of UO₂(cr) to U₄O₉(cr) in granite is not necessary for a considerable increase in uranium solubility. Thermodynamic equilibria are independent of the masses of particular phases but depend only on the appearance or disappear-

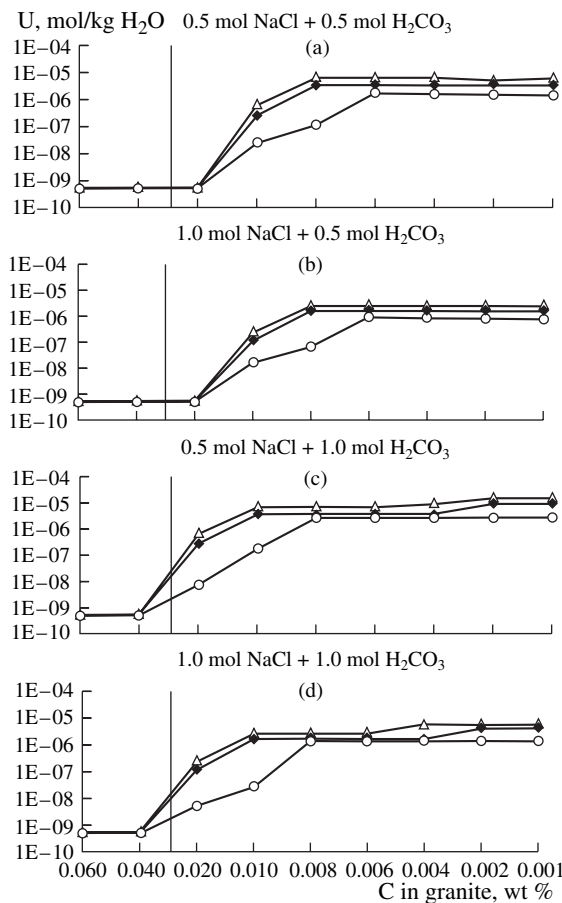


Fig. 9. Uranium release from a granite with background uranium content [31] into solutions of variable composition at temperatures of 250, 200, and 150°C and a pressure of 1 kbar as a function of bulk carbon content in the solid phase of the granite. Diagrams (a–d) correspond to various proportions of NaCl and H₂CO₃ in the solution affecting the granite.

ance of their arbitrary amounts in the system. In their investigation of uranium solubility in natural waters, Barsukov and Borisov [36] demonstrated that a very slight oxidation of UO₂(cr) to U₄O₉(cr) is sufficient to increase the concentration of uranium in the equilibrium aqueous phase by several orders of magnitude.

The same occurs if *carbon content only* is changed in the granite. Figure 9 shows the curves of uranium release into solutions of various compositions from sulfur-free granite with varying carbon contents. The symbols in this diagram are the same as in Fig. 8. It should be emphasized again that the results of modeling are insensitive to the form in which the background amounts of C are introduced into the granite: the equilibrium proportions of its forms of different valence (carbonate, graphite, and methane) are established independent of the initial speciation [33]. It can be seen that in this case, the ore concentrations of uranium in the solution are attained when the content of carbon in the granite is three times lower than the background value. We do not consider here the combined influence

of both components of variable valence (iron should be added to them!) on the behavior of uranium in the granite–solution system. This requires a special de-tailed analysis, which will be performed later. However, it is clear that their simultaneous occurrence in the solid phase should strengthen the effects described here for each of them separately.

The simulation of processes occurring during the pre-uranium period in the Aue granite cupola [1] and action of pore solutions after their migration from the cupola into the ore field showed that tremendous amounts of sulfur (II), ferrous iron, and carbon were removed from the granites of the upper part of the cupola during the formation of the real early quartz and quartz–sulfide veins of Schlemma. This provided favorable geochemical conditions for the partial oxidation of uranium in the granite to U(VI) and replacement of low-soluble U(IV) species by uranyl species. These processes were necessary for the beginning of the extensive migration of uranium from the granite into fissure veins. This is why the U-ore veins of Schlemma and other vein-type deposits are usually formed after seemingly “useless” nonproductive processes, which imperceptibly change with time the behavior of uranium in the granite–solution system.

Could hydrothermal solutions having a temperature of 200°C (average temperature of uranium ore generation) perform themselves this preliminary work, necessary for uranium mobilization and accumulation in veins? In principle, this is, of course, possible but at a much smaller scale. A comparison of Tables 1–3 and 6 shows that from 500 to 300°C the intensity of silica removal decreases by almost an order of magnitude, and the extraction of sulfur and iron from the granite decreases by almost two orders of magnitude. The intensity of the removal of these components further declines to 250–200°C. Therefore, if the solutions started infiltrating through the granite at low *T* and *P*, they would have extracted several orders of magnitude less SiO₂, S(II), and Fe(II) for the same amount of H₂O. This implies that the development of conditions necessary for uranium mobilization would have required *orders of magnitude greater amounts of solutions and orders of magnitude longer times*. The question is whether the available solution resources and time will suffice for the development of favorable conditions for the extensive involvement of uranium into the hydrothermal process. Therefore, the extensive transportation of uranium from granites into the hydrothermal veins among the productive sequence of rocks with a high reducing capacity [30] required *large-scale high-temperature processes*, in the course of which the granite and equilibrium pore solutions were affected by active alteration (including oxidation) and favorable conditions for the subsequent uranium migration were developed. This mechanism operated in Schlemma and other large vein-type uranium deposits. Proceeding from these considerations, we can answer in the affirmative the question of whether the preliminary high-temperature nonuranium processes were necessary for

the formation of considerable amounts of hydrothermal uranium ores. Yes, in our opinion, they were necessary.

The development of preliminary redox conditions in the granite and equilibrium solution was absolutely indispensable for the extraction of considerable masses of uranium and its reprecipitation in veins. And this was the main mission of both premineralization stages of the hydrothermal process at Schlema. Without attaining these conditions, the following steps necessary for uranium mineralization would have been much less pronounced or merely impossible: partial oxidation of uranium previously immobilized in the Aue granite as U(VI) titanates and oxides, dissolution and transportation of considerable amounts of U(VI) from the Aue cupola, and uranium accumulation in the quartz–calcite–pitchblende veins of the deposit at the expense of U(VI) reduction to U(IV) within the productive rock sequence of the Schlema deposit.

DISCUSSION

(1) As was pointed out in [1], our thermodynamic models are not virtual copies of particular objects or phenomena (processes). The models are a tool, in which input parameters can be changed and their influence on the tendencies of the evolution of modeled objects or phenomena can be evaluated. The analysis of these changes allows us to estimate their significance in nature. Because of this, we use a spectrum of solutions rather than a unique “true” solution in our models, such that the reader may appreciate the consequences related to various changes in them. For the same reason, different precipitates were also shown in order to illustrate how variations in the proportion of solution components and T – P conditions are reflected in their compositions, and so on. We consider this more interesting and important than the mechanical choice of a combination of factors providing a model appearing as an exact copy of the target. It should also be taken into account that our modeling is based on the calculation of thermodynamic equilibria toward which the systems tend, although they may not attain the equilibrium states owing to kinetic limitations.

(2) The main essence and main material evidence for the extensive geochemical action of the premineralization stages of the hydrothermal process at Schlema are, *first*, very weak and seemingly unimportant changes in the mineral and chemical compositions of tremendous masses of granite in the upper part of the Aue cupola [1, 17]; *second*, the intense removal of metals, including uranium from this part of the cupola [1, 17, 18]; and *third*, the formation of fissure quartz and quartz–sulfide veins of Schlema above the cupola, where many elements removed from the granite were concentrated [2, 3]. In this paper we continue to analyze causal links between these three sides of premineralization processes, which, in turn, are manifested in a more discrete sequence of events. Based on a series of models, we traced the logical sequence and interrelations of

all the phenomena occurring successively at Schlema and below it, in the Aue granite before the formation of primary uranium ores: the inflow of nonequilibrium solutions into the upper part of the cooling Aue granite cupola (above the –1260 m horizon relative to the MS level) → their interaction with the granite (granite “flushing”) at relatively high T and P → slight changes in the initial composition of granite (its “dispersed muscovitisation”) caused by the solutions → formation, owing to these reactions, of thermal pore solutions equilibrated with the granite and saturated in silica and granitic ore components → the disturbance of physicochemical equilibria in the pore solutions during their movement along fractures into a colder zone, owing to both a decrease in T and P and reaction with the environment (pore solutions are part of this environment) → the precipitation of gangue and ore materials in the free space of fissures (formation of early pre-uranium quartz and quartz–sulfide veins). It was shown that this logical sequence of interrelated phenomena predated the extensive development of U mineralization at Schlema.

(3) Since quartz is the most abundant mineral in the premineralization veins, silica plays the key role in the verification of models: saturation of pore solutions in SiO_2 at various P – T conditions and silica loss from the solutions in response to changes in these conditions. The plausibility of models for the granite–solution system can be assessed by comparing the silica behavior in them with the available experimental data. The solubility of silica in our models is in agreement with experiments [14, 15]. Many other experimentally observed features of quartz dissolution were also reflected in the results of modeling. For instance, according to Anderson and Burnham [37], the solubility of quartz in supercritical water (700°C and 4 kbar or 600°C and 3 kbar) decreases somewhat with the addition of chlorides. Our models showed higher silica contents in pure water compared with chloride-bearing solutions, and this effect was traced at least to 300°C and 2 kbar. The classical diagram of G. Kennedy exhibits an increase in silica solubility with increasing pressure from 150 to 1750 bar. This effect was observed in the models under the same conditions and at higher pressures by comparing quartz solubilities at 3 and 2 kbar. As was pointed out by Holland [14], “The near-independence of the solubility of the silica polymorphs of ionic strength and pH permits us to discuss the solution and deposition of quartz in hydrothermal systems without undue worry concerning the effects of other dissolved species in solution.” As was shown in the present study, the model pore solutions of substantially different salt compositions show only minor differences in the concentration of dissolved SiO_2 under the same P – T conditions (Fig. 1), and so on. These and other examples of agreement with experimental data suggest the plausibility of our models with respect to silica dissolution from the granite.

The same can be said of the precipitation of silica from solutions during cooling and decompression. According to the above estimates, the formation of the early quartz vein of Schlema (about E+07–E+08 t SiO_2)

owing to the cooling of high-temperature solutions from 450 to 350°C and lower temperatures requires (for a precipitation of 3 g SiO₂ per 1 kg H₂O) no less than 4E+12–4E+13 t of such solutions. The obtained specific release of SiO₂ into the precipitate and the mass of solutions necessary for the formation of a certain amount of quartz are in agreement with the estimates of Holland [14] (1E+05 t of quartz can be deposited from 5E+08 t of solution). Holland argued that “this calculation is not very sensitive to the assumed value of the thermal gradient and the pressure gradient.” This agreement also supports the reliability of values obtained in our models. In fact, there could have been no other result, because the thermodynamic constants used in our models were calculated from the aforementioned data and other experiments consistent with them. If we were interested in the behavior of silica only, the modeling would have been of little use, because all the necessary relationships could have been merely derived from reliable experimental data.

Since reliable results were obtained for silica, which is one of the major components of premineralization processes, it can be suggested that the models are valid for other components, which participated in these processes and were strictly connected to silica by thermodynamic relations.

(4) Compared with the quartz stage, the formation of quartz–sulfide veins is in essence a very weak development and accomplishment of the large-scale process of the extraction of silica and accompanying components from the granites of the upper part of the Aue cupola and their reprecipitation within the ore body. As was shown by the models, the formation of the mineral assemblages of these veins could be related to solution cooling and decompression (minor early quartz–hematite assemblage and predominant quartz–sulfide assemblage) or involved reactions with S(II)-bearing pore solutions from the wallrocks of Schlema (quartz–base metal assemblage).

In general, two features of these two premineralization stages of the hydrothermal process deserve special attention. The compositions and properties of the high-temperature (500–400°C) solutions forming the veins of these two stages were controlled by chemical reactions between the granite and water phase percolating through it, which tended toward mutual equilibrium. The draining of the Aue granite cupola by fissure systems transported these solutions upward into the outlines of the Schlema ore field and a colder part of the section. The cooling of high-temperature solutions in this cold zone resulted in the precipitation of a solid phase corresponding to the average composition of the real early quartz and some quartz–sulfide veins of Schlema. This allows us to suggest that a *physical factor* was responsible for the formation of the early veins, namely, heat exchange between hot solutions percolating through the granite and the colder rocks of the ore field. Exchange chemical reactions between such high-

temperature solutions with the environment played only a minor role. The dynamics of such heat exchange processes resulting in the cooling of hot solutions percolating through fissures and wallrock heating near the fissures was modeled by Pampura et al. [38], Pek et al. [39], and others. Subsequently, owing to the considerable depletion of granite-derived solutions in sulfide sulfur at temperatures of ≤350–300°C, the *chemical factor*, i.e., mixing of solutions of different origins and properties and exchange reactions between them, became important for the precipitation of base-metal sulfides forming the final assemblages of the quartz–sulfide veins.

(5) Of particular importance for the understanding of the premineralization processes of Schlema is the fact that even at the slight alteration of the granite by thermal solutions it was accompanied by the extraction of tremendous amounts of silica and other components. We showed above that the amounts of sulfur and iron removed from the granite were comparable with that of silica and discussed the geochemical significance of this observation. The data of Tables 1–3 and 6 allow us to estimate the removal of other major components from the granite. They have different fates, but after the transportation of the high-temperature solutions into the cold zones of the section, a certain fraction of each component was fixed in some newly formed solid phase producing a quartz-dominating precipitate identical or similar in composition to the vein material of the real quartz and quartz–sulfide veins.

The extraction of metals from a weakly altered granite is not the discovery of modeling. This process was documented by the analyses of the largest available sets of samples [1, 17, 18]. Statistically reliable data suggest that, compared with the lower part of the Aue cupola, the granites of the upper part contain only 74% of uranium and sulfur, 63% of zinc, 40% of lead, etc. The content of any ore element decreased during the weak alteration of granites (“dispersed muscovitization”) at the expense of their progressive leaching by solutions percolating through the granite.

(6) The results of our simulation demonstrated that the extraction of uranium by solutions from the *unaltered* Aue granite is improbable, and the transformation of uranium into a mobile state required *preliminary granite alteration*. This conclusion is not surprising. As early as 1996, in our paper with Ryzhenko and Knyazeva on the chemical characteristics of the granite–water system [32] and in a later publication [34], we stated that the redox potential of pore solutions from the average granite composition (classical granite after R.O. Daly and A.N. Zavaritskii) at temperatures of <400°C is *rather low*, similar to that of pore solutions from pyroxenite (!), and much lower than that of pore solutions from syenite, diorite, and gabbro. This is probably related to higher background contents of variable-valence S and C in the granite compared with other igneous rocks. When this study was discussed

with N.P. Laverov, he advised to draw the attention of geologists to the fact that this property of granite may have significant consequences for the fate of many dispersed ore elements, including uranium, and that it deserves further investigation. Such preliminary additional information derived from the trilateral discussion of the problem was published in *Doklady, Earth Sciences* [39].

Much earlier, in the 1950s–1960s, when the remarkable idea of L.V. Tauson on the presence of free forms of uranium and other metals in granitoids attracted considerable attention, thousands of analyses were reported demonstrating that diluted ammonium carbonate (or chloride) solutions can extract up to 90% of uranium from rocks. And this result was achieved *without the decomposition of the major minerals* of the granite: the absence of alkalis (indicator of the preservation of feldspars) and divalent bases (indicator of the preservation of mafic minerals) in the solutions was strictly observed. True is that a drop of oxidizer (for instance, H₂O₂) was added to the solution to increase the extraction of uranium. Our models demonstrated that the same process takes place in nature by the example of the Aue granite cupola. The only difference is that there was no addition of an artificial oxidizer, and the same effect was produced by the water of premineralization processes, which caused almost negligible alterations in the granite but gradually oxidized it and equilibrium pore solutions. Similar to the experiments of Tauson, the extraction of tremendous amounts of uranium from the granite occurred without the significant decomposition of its major phases.

It can be stated that the dependence of uranium extraction from granite by aqueous solutions on the content of variable-valence major (Fe and Mn) and volatile components (S, C, to a smaller extent As, Se, and others) remains an important geochemical issue, which contains many intriguing features and deserves a comprehensive investigation and discussion by experts in various disciplines.

ACKNOWLEDGMENTS

This study was financially supported by the Russian Foundation for Basic Research, project no. 05-05-65098.

REFERENCES

1. Vikt. L. Barsukov, "Modeling of Geochemical Processes That Occurred during the Formation of the Schlema Deposit, Erzgebirge. I. Synmineralization Processes in the Aue Granites," *Geokhimiya*, No. 6, 643–665 (2006) [*Geochem. Int.* **44**, 591–612 (2006)].
2. B. P. Vlasov, L. V. Matyushin, and G. B. Naumov, "Schlema–Alberoda Vein-Type Uranium Deposit, Erzgebirge," *Geol. Rudn. Mestorozhd.*, No. 3, 205–221 (1993).
3. B. N. Acheev, Extended Abstract of Candidate's Dissertation in Geology and Mineralogy (Aue, 1968).
4. Yu. V. Shvarov, "Algorithmization of the Numeric Equilibrium Modeling of Dynamic Geochemical Processes," *Geokhimiya* **37**, 646–652 (1999) [*Geochem. Int.* **37**, 571–576 (1999)].
5. Yu. V. Shvarov and E. N. Bastrakov, *HCh: A Software Package for Geochemical Equilibrium Modeling (User's Guide)* (Australian Geological Survey Organization, Canberra, 1999).
6. G. B. Naumov, N. T. Sokolova, L. V. Matyushin, and B. I. Malyshev, "Role of Contact Metamorphism in the Formation of Uranium Mineralization," *Geokhimiya*, No. 8, 1113–1128 (1986).
7. D. Harzer, "Isotopengeochemische Untersuchungen (¹⁸O und ¹³C) an hydrothermalen Mineralen aus Ganglagerstätten der DDR," *Freib. Forschungs* **C247** (1970).
8. *Problems of Metasomatism* (Nedra, Moscow, 1970) [in Russian].
9. C. J. Burton and H. C. Helgeson, "Calculation of the Chemical and Thermodynamic Consequences of Differences between Fluid and Geostatic Pressure in Hydrothermal Systems," *Am. J. Sci.* **283A**, 540–588 (1983).
10. B. W. D. Yardley, "On Some Quartz–Plagioclase Veins in the Connemara Schists, Ireland," *Geol. Mag.* **112**, 183–190 (1975).
11. J. V. Walther and H. C. Helgeson, "Calculation of the Thermodynamic Properties of Aqueous Silica and the Solubility of Quartz and Its Polymorphs at High Pressures and Temperatures," *Am. J. Sci.* **277**, 1315–1351 (1977).
12. *Fluid–Rock Interaction during Metamorphism*, Ed. By J. V. Walther and B. J. Wood (Springer, New York, 1986; Mir, Moscow, 1989).
13. N. T. Sokolova and B. N. Acheev, "Reasons for the Localization of Uranium Mineralization in the Contact Metamorphic Aureoles of Granitoids," *Geokhimiya*, No. 1, 110–123 (1972).
14. H. D. Holland, "Gangue Minerals in Hydrothermal Deposits," in *Geochemistry of Hydrothermal Ore Deposits*, Ed. By H. L. Barnes (Holt, Rinehart and Winston, New York, 1967; Mir, Moscow, 1970), pp. 382–432.
15. H. D. Holland and S. D. Malinin, "Solubility and Occurrence of Non-Ore Minerals," in *Geochemistry of Hydrothermal Ore Deposits*, Ed. by H. L. Barnes (Wiley, New York, 1979; Mir, Moscow, 1982), pp. 461–508.
16. G. P. Zarskii, "The Conditions of the Nonequilibrium Silicification of Rocks and Quartz Vein Formation during Acidic Metasomatism," *Geol. Rudn. Mestorozhd.* **41**, 294–307 (1999) [*Geol. Ore Dep.* **41**, 262–275 (1999)].
17. Vikt. L. Barsukov, N. T. Sokolova, and O. M. Ivanitskii, "Metals, Arsenic, and Sulfur in the Aue and Eibenstock Granites, Erzgebirge," *Geokhimiya* (in press).
18. Vikt. L. Barsukov, N. T. Sokolova, and O. M. Ivanitskii, "Distribution of U, Th, and K in Granites of the Aue and Eibenstock Massifs, Erzgebirge, Germany," *Geokhimiya* **34**, 1157–1174 (1996) [*Geochem. Int.* **34**, 1041–1056 (1996)].
19. *Metallogenetische Karte Erzgebirges*, Zusammengestellt durch J. Wasternack in Zusammenarbeit mit G. Tis-

- chendorf (Berlin), K. Posmorny and M. Stempok (Praha) (1974).
20. G. Tischendorf, J. Wasternack, H. Bolduan, and E. Bein, "Zur Lage der Granitoberfläche im Erzgebirge und Fogtland," *Z. Angew. Geologie* **11**, 410–425 (1965).
 21. Yu. M. Dymkov, *Uranium Mineralization of the Erzgebirge* (Atomizdat, Moscow, 1960) [in Russian].
 22. N. T. Sokolova, "Iron in Wallrock Metasomatism at Uranium Deposits," *Geokhimiya*, No. 11, 1335–1342 (1970).
 23. A. G. Betekhtin, "Hydrothermal Solutions, Their Nature, and Ore Formation," in *Main Problems in the Concept of Magmatic Ore Deposits* (AN SSSR, Moscow, 1953), pp. 122–275.
 24. V. I. Smirnov, *Geology of Mineral Resources* (Nedra, Moscow, 1976) [in Russian].
 25. B. J. Skinner, "The Many Origins of Hydrothermal Ore Deposits," in *Geochemistry of Hydrothermal Ore Deposits*, Ed. by H. L. Barnes (Wiley, New York, 1979; Mir, Moscow, 1982), pp. 1–21.
 26. A. A. Pek, *Dynamics of Juvenile Solutions* (Nauka, Moscow, 1969) [in Russian].
 27. A. A. Pek, D. I. Peresun'ko, and I. I. Krashin, "Faults and Flow of Hydrothermal Solutions," *Geol. Rudn. Mestorozhd.*, No. 5, 320–334 (1970).
 28. Vikt. L. Barsukov and A. A. Pek, "Hydrodynamic Aspects of Ore Formation and Wallrock Alteration," in *Reports of Soviet Geologists at the 36th IGC. Geochemistry and Mineralogy* (Nauka, Moscow, 1980), pp. 61–70 [in Russian].
 29. N. P. Laverov, Vikt. L. Barsukov, V. I. Mal'kovskii, and A. A. Pek, "Hydrodynamic Conditions of Solution Mixing during Formation of Cross-Cutting Veins in Bedded Sequences," *Geol. Rudn. Mestorozhd.*, No. 4, 334–357 (1995).
 30. Vikt. L. Barsukov, "Pore Solutions in the Rocks of the Schlemma Uranium Deposit, Erzgebirge, and Their Role in Ore Formation," *Geokhimiya*, No. 5, 503–524 (2004) [*Geochem. Int.* **42**, 428–448 (2004)].
 31. A. N. Zavaritskii, *Igneous Rocks* (Akad. Nauk SSSR, Moscow, 1956) [in Russian].
 32. B. N. Ryzhenko, Vikt. L. Barsukov, and S. N. Knyazeva, "Chemical Characteristics (Composition, pH, and Eh) of a Rock–Water System: 1. The Granitoids–Water System," *Geokhimiya*, No. 5, 436–454 (1996) [*Geochem. Int.* **34**, 390–407 (1996)].
 33. B. N. Ryzhenko, Vikt. L. Barsukov, and S. N. Knyazeva, "Chemical Characteristics (Composition, pH, and Eh) of the Rock–Water System: II. Diorite (Andesite)–Water and Gabbro (Basalt)–Water Systems," *Geokhimiya*, No. 12, 1227–1254 (1997) [*Geochem. Int.* **35**, 1089–1115 (1997)].
 34. Vikt. L. Barsukov and B. N. Ryzhenko, "Temperature Evolution of Pore Solutions in Equilibrium with Rocks of Various Silica Contents," *Geol. Rudn. Mestorozhd.* **43**, 208–226 (2001) [*Geol. Ore Dep.* **43**, 184–201 (2001)].
 35. A. P. Vinogradov, "Average Abundances of Chemical Elements in the Main Types of Igneous Rocks of the Earth's Crust," *Geokhimiya*, No. 7, 555–571 (1962).
 36. Vikt. L. Barsukov and M. V. Borisov, "Models of Uranium Dissolution in Natural Waters of Various Compositions," *Geokhimiya*, No. 1, 43–69 (2003) [*Geochem. Int.* **41**, 38–63 (2003)].
 37. G. M. Anderson and C. W. Burnham, "The Solubility of Quartz in Supercritical Water," *Am. J. Sci.* **263**, 494–511 (1965).
 38. V. D. Pampura, V. N. Kochergin, and O. A. Balyshev, *Physical–Mathematical Models of Natural Hydrothermal Systems* (Nauka, Moscow, 1973) [in Russian].
 39. A. A. Pek, V. I. Mal'kovskii, P. L. Arsen'ev, and D. N. Topor, "Temperature Distribution in a Vertical Fault during the Ascending Movement of Hydrothermal Solution," *Geol. Rudn. Mestorozhd.*, No. 6, 93–96 (1987).
 40. N. P. Laverov, B. N. Ryzhenko, and Vikt. L. Barsukov, "Redox Potential of Hydrothermal Systems in Granitic Rocks," *Dokl. Ross. Akad. Nauk* **349**, 243–248 (1996) [*Dokl. Earth Sci.* **349**, 873–877 (1996)].